

1 **SYNERGY BETWEEN SATELLITE OBSERVATIONS OF SOIL MOISTURE**  
2 **AND WATER STORAGE ANOMALIES FOR RUNOFF ESTIMATION**

3 Stefania Camici <sup>(1)</sup>, Gabriele Giuliani <sup>(1)</sup>, Luca Brocca <sup>(1)</sup>, Christian Massari <sup>(1)</sup>, Angelica Tarpanelli  
4 <sup>(1)</sup>, Hassan Hashemi Farahani <sup>(2)</sup>, Nico Sneeuw <sup>(2)</sup>, Marco Restano <sup>(3)</sup>, Jérôme Benveniste <sup>(4)</sup>

5 *(1) National Research Council, Research Institute for Geo-Hydrological Protection, Perugia, Italy ([s.camici@irpi.cnr.it](mailto:s.camici@irpi.cnr.it))*

6 *(2) Institute of Geodesy, University of Stuttgart, Geschwister-Scholl-Straße 24D, 70174 Stuttgart, Germany*

7 *(3) SERCO c/o ESA-ESRIN, Largo Galileo Galilei, Frascati, 00044, Italy*

8 *(4) European Space Agency, ESA-ESRIN, Largo Galileo Galilei, Frascati, 00044, Italy*

9

10

11

12

13

14

15

16

17

18

**November 2020**

19

Submitted to:

20

\* Correspondence to: Ph.D. Stefania Camici, Research Institute for Geo-Hydrological Protection, National Research Council, Via della Madonna Alta 126, 06128 Perugia, Italy. Tel: +39 0755014419 Fax: +39 0755014420 E-mail: [stefania.camici@irpi.cnr.it](mailto:stefania.camici@irpi.cnr.it).

## 21    **ABSTRACT**

22    This paper presents an innovative approach, STREAM - SaTellite based Runoff Evaluation And  
23    Mapping - to derive daily river discharge and runoff estimates from satellite soil moisture,  
24    precipitation and terrestrial water storage anomalies observations. Within a very simple model  
25    structure, the first two variables (precipitation and soil moisture) are used to estimate the quick-flow  
26    river discharge component while the terrestrial water storage anomalies are used for obtaining its  
27    complementary part, i.e., the slow-flow river discharge component. The two are then summed up to  
28    obtain river discharge and runoff estimates.

29    The method is tested over the Mississippi river basin for the period 2003-2016 by using Tropical  
30    Rainfall Measuring Mission (TRMM) Multi-satellite Precipitation Analysis (TMPA) precipitation  
31    data, European Space Agency Climate Change Initiative (ESA CCI) soil moisture data and Gravity  
32    Recovery and Climate Experiment (GRACE) terrestrial water storage data. Despite the model  
33    simplicity, relatively high-performance scores are obtained in river discharge simulations, with a  
34    Kling-Gupta efficiency index greater than 0.65 both at the outlet and over several inner stations used  
35    for model calibration highlighting the high information content of satellite observations on surface  
36    processes. Potentially useful for multiple operational and scientific applications (from flood warning  
37    systems to the understanding of water cycle), the added-value of the STREAM approach is twofold:  
38    1) a simple modelling framework, potentially suitable for global runoff monitoring, at daily time scale  
39    when forced with satellite observations only, 2) increased knowledge on the natural processes, human  
40    activities and on their interactions on the land.

41

42    Key words: satellite products, soil moisture, water storage variations, conceptual hydrological  
43    modelling, rainfall-runoff modelling, Mississippi.

## 44 1. INTRODUCTION

45 Spatial and temporal continuous river discharge monitoring is paramount for improving the  
46 understanding of the hydrological cycle, for planning human activities related to water use as well as  
47 to prevent/mitigate the losses due to extreme flood events. To accomplish these tasks, runoff and river  
48 discharge data, which represents the aggregated signal of runoff (Fekete et al., 2012), should be  
49 available at adequate spatial/temporal resolution, i.e., at basin scale (basin area larger than 10'000  
50 km<sup>2</sup>) and at monthly time step for water resources management and drought monitoring up to grid  
51 scale (few km)/(sub-) daily time step for flood prediction. The accurate continuous (in space and  
52 time) runoff and river discharge estimation at finer spatial/temporal resolution is still a big challenge  
53 for hydrologists.

54 Traditional in situ observations of river discharge, even if generally characterized by high temporal  
55 resolution (up to sub-hourly time step), typically offer little information on the spatial distribution of  
56 runoff within a watershed. Moreover, river discharge observation networks suffer from many  
57 limitations such as low station density and often incomplete temporal coverage, substantial delay in  
58 data access and large decline in monitoring capacity (Vörösmarty et al. 2002). Paradoxically, this  
59 latter issue is exacerbated in developing nations (Crochemore et al, 2020), where the knowledge of  
60 the terrestrial water dynamics deserves greater attention due to huge damages to settlements and  
61 especially the loss of human lives that occurs regularly.

62 This precarious situation has led to growing interest in finding alternative solutions, i.e., model-based  
63 or observation-based approaches, for runoff and river discharge monitoring. Model-based  
64 approaches, based on the mathematical description of the main hydrological processes (e.g., water  
65 balance models, WBMs, global hydrological models, GHMs, e.g., Döll et al., 2003 or, increasing in  
66 complexity, land surface models, LSM, e.g., Balsamo et al., 2009; Schellekens et al., 2017), are able  
67 to provide comprehensive information on a large number of relevant variables of the hydrological  
68 cycle including runoff and river discharge at very high temporal and spatial resolution (up to hourly

69 sampling and 0.05° grid scale). However, the values of simulated water balance components rely on  
 70 a massive parameterization of the soil, vegetation and land parameters, which is not always realistic,  
 71 and are strongly dependent on the GHM/ LSM models used, analysis periods (Wisser et al., 2010)  
 72 and climate forcings selected (e.g Haddeland et al., 2012; Gudmundsson et al., 2012a, b; Prudhomme  
 73 et al., 2014; Müller Schmied et al., 2016).  
 74 Alternatively, the observation-based approaches exploit machine learning techniques and a  
 75 considerable amount of data to describe the physics of the system (i.e. hydraulic and/or hydrologic  
 76 phenomena, Solomatine and Ostfeld, 2008) with only a limited number of assumptions. Besides being  
 77 simpler than model-based approaches, these approaches still present some limitations. At first, as they  
 78 rely on a considerable amount of data describing the modelled system's physics, the spatial/temporal  
 79 extent and the uncertainty of the resulting dataset is determined by the spatial/temporal coverage and  
 80 the accuracy of the forcing data (e.g., see E-RUN dataset, Gudmundsson and Seneviratne, 2016;  
 81 GRUN dataset, Ghiggi et al., 2019; FLO1K dataset, Barbarossa et al., 2018). Additional limitations  
 82 stem from the employed method to estimate runoff. Indeed, random forests such as employed in  
 83 Gudmundsson and Seneviratne, 2016, like other machine learning techniques, are powerful tools for  
 84 data driven modeling, but they are prone to overfitting, implying that noise in the data can obscure  
 85 possible signals (Hastie et al., 2009). Moreover, the influence of land parameters on continental-scale  
 86 runoff dynamics is not taken into account as the underlying hypothesis is that the hydrological  
 87 response of a basin exclusively depend on present and past atmospheric forcing. It is easy to  
 88 understand that this assumption will only be valid in certain circumstances and might lead to  
 89 problems, e.g., over complex terrain (Orth and Seneviratne, 2015) or in cases of human river flow  
 90 regulation (Ghiggi et al., 2019).  
 91 Remote sensing can provide estimates of nearly all the climate variables of the global hydrological  
 92 cycle including soil moisture (e.g., Wagner et al., 2007; Seneviratne et al., 2010), precipitation  
 93 (Huffman et al., 2014) and total terrestrial water storage (e.g., Houborg et al., 2012; Landerer and  
 94 Swenson, 2012; Famiglietti and Rodell, 2013). It has undeniably changed and improved dramatically

95 the ability to monitor the global water cycle and, hence, runoff. By taking advantage of satellite  
96 information, some studies tried to develop methodologies able to optimally produce multivariable  
97 datasets from the fusion of in situ and satellite-based observations (e.g., Rodell et al., 2015; Zhang et  
98 al., 2018; Pellet et al., 2019). Other studies exploited satellite observations of hydrological variables,  
99 e.g., precipitation (Hong et al., 2007), soil moisture (Massari et al., 2014), and geodetic variables (e.g.,  
100 Sneeuw et al., 2014; Tourian et al., 2018) to monitor single components of the water cycle in an  
101 independent way.

102 Although the majority of these studies provide runoff and river discharge data at basin scale and  
103 monthly time step, they deserve to be recalled here as important for the purpose of the present study.  
104 In particular, Hong et al. (2007) presented a first attempt to obtain an approximate but quasi-global  
105 annual streamflow dataset, by incorporating satellite precipitation data in a relatively simple rainfall-  
106 runoff simulation approach. Driven by the multiyear (1998-2006) Tropical Rainfall Measuring  
107 Mission Multi-satellite Precipitation Analysis, runoff was independently computed for each global  
108 land surface grid cell through the Natural Resources Conservation Service (NRCS) runoff curve  
109 number (CN) method (NRCS, 1986) and subsequently routed to the watershed outlet to simulate  
110 streamflow. The results, compared to the in situ observed discharge data, demonstrated the potential  
111 of using satellite precipitation data for diagnosing river discharge values both at global scale and for  
112 medium to large river basins. If, on the one hand, the work of Hong et al. (2007) can be considered  
113 as a pioneer study, on the other hand it presents a serious drawback within the NRCS-CN method  
114 that lacks a realistic definition of the soil moisture conditions of the catchment before flood events.  
115 This aspect is not negligible, as it is well established that soil moisture is paramount in the partitioning  
116 of precipitation into surface runoff and infiltration inside a catchment (Brocca et al., 2008). In  
117 particular, for the same rainfall amount but different values of initial soil moisture conditions,  
118 different flooding effects can occur (see e.g. Crow et al., 2005; Brocca et al., 2008; Berthet et al.,  
119 2009; Merz and Blochl, 2009; Tramblay et al., 2010). On this line following Brocca et al. (2009),  
120 Massari et al. (2016) presented a very first attempt to estimate global streamflow data by using

121 satellite Soil Moisture Active and Passive (SMAP, Entekhabi et al., 2010) and Global Precipitation  
122 Measurement (GPM, [Huffman et al., 2019](#)) products. Although the validation was carried out by  
123 routing the monthly surface runoff only in a single basin in Central Italy, the obtained results  
124 suggested to dedicate additional efforts in this direction.

125 Among the studies that use satellite observations of hydrological variables for runoff estimation, the  
126 hydro-geodetic approaches are undoubtedly worth mentioning, see e.g., ([Sneeuw et al., 2014](#)) for a  
127 comprehensive overview or [Lorenz et al. \(2014\)](#) for an analysis of satellite-based water balance  
128 misclosures with discharge as closure term. In particular, the satellite mission Gravity Recovery And  
129 Climate Experiment (GRACE), which observed the temporal changes in the gravity field, has given  
130 a strong impetus to satellite-driven hydrology research ([Tapley et al., 2019](#)). Since temporal gravity  
131 field variations over the continents imply water storage change, GRACE was the first remote sensing  
132 system to provide observational access to deeper groundwater storage. The relation between GRACE  
133 groundwater storage change and runoff was characterized by [Riegger and Tourian \(2014\)](#), which even  
134 allowed the quantification of absolute drainable water storage over the Amazon ([Tourian et al., 2018](#)).  
135 In essence the storage-runoff relation describes the gravity-driven drainage of a basin and, hence, the  
136 slow-flow processes. Due to GRACE's spatial-temporal resolution, runoff and river discharge are  
137 generally available for large basins ( $>160'000 \text{ km}^2$ ) and at monthly time step.

138 Based on the above discussion, it is clear that each approach presents strengths and limitations that  
139 enable or hamper the runoff and river discharge monitoring at finer spatial and temporal resolutions.  
140 In this context, this study presents an attempt to find an alternative method to derive daily river  
141 discharge and runoff estimates at  $\frac{1}{4}$  degree spatial resolution exploiting satellite observations and the  
142 knowledge of the key mechanisms and processes that act in the formation of runoff, i.e., the role of  
143 soil moisture in determining the response of a catchment to precipitation. For that, soil moisture,  
144 precipitation and terrestrial water storage anomalies (TWSA) observations are used as input into a  
145 simple modelling framework named STREAM v1.3 (SaTellite based Runoff Evaluation And  
146 Mapping, version 1.3). Unlike classical land surface models, STREAM exploits the knowledge of the

147 system states (i.e., soil moisture and TWSA) to derive river discharge and runoff, and thus it 1) skips  
148 the modelling of the evapotranspiration fluxes which are known to be a non-negligible source of  
149 uncertainty (Long et al. 2014), 2) limits the uncertainty associated with the over-parameterization of  
150 soil and land parameters and 3) implicitly takes into account processes, mainly human-driven (e.g.,  
151 irrigation, change in the land use), that might have a large impact on the hydrological cycle and hence  
152 on runoff.

153 The detailed description of the STREAM v1.3 model is given in section 4. The collected datasets and  
154 the experimental design for the Mississippi River Basin (section 2) are described in sections 3 and 5,  
155 respectively. Results, discussion and conclusions are drawn in section 6, 7 and 8, respectively.

## 156 **2. STUDY AREA**

157 The STREAM v1.3 model presented here has been tested and validated over the Mississippi River  
158 basin. With a drainage area of about 3.3 million km<sup>2</sup>, the Mississippi River basin is the fourth largest  
159 watershed in the world, bordered to the West by the crest of the Rocky Mountains and to the East by  
160 the crest of the Appalachian Mountains. According to the Köppen climate classification, the climate  
161 is subtropical humid over the southern part of the basin, continental humid with hot summer over the  
162 central part, continental humid with warm summer over the eastern and norther parts, whereas a  
163 semiarid cold climate affects the western part. The average annual air temperature across the  
164 watershed ranges from 4°C in the West to 6°C in the East. On average, the watershed receives about  
165 900 mm/year of precipitation (77% as rainfall and 23% as snowfall), more concentrated in the eastern  
166 and southern portions of the basin with respect to its northern and western part (Vose et al., 2014).

167 The river flow has a clear natural seasonality mainly controlled by spring snowmelt (coming from  
168 the Missouri and the Upper Mississippi, the eastern and the upper part of the basin, respectively, Dyer  
169 2008) and by heavy precipitation exceeding the soil moisture storage capacity (mostly occurring in  
170 the eastern and southern part of the basin, Berghuijs et al., 2016). The basin is also heavily regulated  
171 by the presence of large dams (Global Reservoir and Dam Database GRanD, Lehner et al., 2011)

most of them located on the Missouri river. In particular, the river reach between Garrison and Gavins Point dams is the portion of the Missouri river where the large main-channel dams have the greatest impact on river discharge providing a substantial reduction in the annual peak floods, an increase on low flows and a reduction on the overall variability of intra-annual discharges (Alexander et al., 2012). The annual average of Mississippi river discharge at the Vicksburg outlet section is equal to  $17'500 \text{ m}^3/\text{s}$  (see Table 1). Given the variety of climate and topography across the Mississippi River basin, it is a good candidate to test the suitability of the STREAM v1.3 model for river discharge and runoff simulation.

### 3. DATASETS

The datasets used in this study include in situ observations, satellite products and model outputs. The first two datasets have been used as input data to the STREAM v1.3 model. Conversely, the model outputs are used as a benchmark to validate the performance of the STREAM v1.3 model.

#### 3.1 In situ Observations

In situ observations comprise air temperature ( $T_{\text{air}}$ ) and river discharge data ( $Q$ ). For  $T_{\text{air}}$  data the Climate Prediction Center (CPC) Global Temperature data developed by the American National Oceanic and Atmospheric Administration (NOAA) using the optimal interpolation of quality-controlled gauge records of the Global Telecommunication System (GTS) network (Fan et al., 2008) have been used. The dataset, downloadable at (<https://psl.noaa.gov/data/gridded/data.cpc.globaltemp.html>) is available on a global regular  $0.5^\circ \times 0.5^\circ$  grid, and provides daily maximum ( $T_{\text{max}}$ ) and minimum ( $T_{\text{min}}$ ) air temperature data from 1979 to present. The daily average air temperature data have been generated as the mean of  $T_{\text{max}}$  and  $T_{\text{min}}$  of each day.

Daily  $Q$  data over the study basins have been taken from the Global Runoff Data Center (GRDC, [https://www.bafg.de/GRDC/EN/Home/homepage\\_node.html](https://www.bafg.de/GRDC/EN/Home/homepage_node.html)). In particular, 11 gauging stations located along the main river network of the Mississippi River basin have been selected to represent



the spatial distribution of runoff over the basin. The location of these gauging stations along with relevant characteristics (e.g., the upstream basin area, the mean annual river discharge and the presence of upstream dams) are summarized in Table 1. As it can be noted, mean annual river discharge ranges from 141 to 17'500 m<sup>3</sup>/s, and 3 out 11 sections are located downstream big dams (Lehner et al., 2011). In particular, Garrison (the fifth-largest earthen dam in the world), Gavins Point and Kanopolis dams located downstream section 1, 2 and 5 respectively (see Figure 3 and Table 1), are three large dams with a maximum storage of 29'383×10<sup>9</sup> m<sup>3</sup>, 0.607×10<sup>9</sup> m<sup>3</sup>, and 1.058×10<sup>9</sup> m<sup>3</sup> respectively.

### 3.2 Satellite Products

Satellite products include observations of precipitation (*P*), soil moisture and TWSA. The satellite *P* dataset used in this study is the Multi-satellite Precipitation Analysis 3B42 Version 7 (TMPA 3B42 V7) estimate produced by the National Aeronautics and Space Administration (NASA) as the 0.25°×0.25° quasi-global (50°N-S) gridded dataset. The TMPA 3B42 V7 is a gauged-corrected satellite product, with a latency period of two months after the end of the month of record, available at 3h sampling interval from 1998 to present (2020). Major details about the *P* dataset, downloadable from <http://pmm.nasa.gov/data-access/downloads/trmm>, can be found in Huffman et al. (2007). Soil moisture data have been taken from the European Space Agency Climate Change Initiative (ESA CCI) Soil Moisture project (<https://esa-soilmoisture-cci.org/>) that provides a surface soil moisture product (referred to first 2-3 centimeters of soil) continuously updated in term of spatial-temporal coverage, sensors and retrieval algorithms (Dorigo et al., 2017). In this study, the daily combined ESA CCI soil moisture product v4.2 is used, that is available at global scale with a grid spacing of 0.25°, for the period 1978-2016. TWSA have been obtained from the Gravity Recovery And Climate Experiment (GRACE) satellite mission. Here we employ the NASA Goddard Space Flight Center (GSFC) global mascon model, i.e., Release v02.4, (Luthcke et al. 2013). It has been produced based on the mass concentration

(mascon) approach. The model provides surface mass densities on a monthly basis. Each monthly solution represents the average of surface mass densities within the month, referenced at the middle of the corresponding month. The model has been developed directly from GRACE level-1b K-Band Ranging (KBR) data. It is computed and delivered as surface mass densities per patch over blocks of approximately  $1^{\circ} \times 1^{\circ}$  or about 12'000 km<sup>2</sup>. Although the mascon size is smaller than the inherent spatial resolution of GRACE, the model exhibits a relatively high spatial resolution. This is attributed to a statistically optimal Wiener filtering, which uses signal and noise full covariance matrices. This allows the filter to fine tune the smoothing in line with the signal-to-noise ratio in different areas. That is, the less smoothing, the higher signal-to-noise ratio in a particular area and vice versa. This ensures that the filtering is minimal and aggressive smoothing is avoided when unnecessary. Further details of such a filter can be found in Klees et. al (2008). Importantly, the coloured (frequency-dependent) noise characteristic of KBR data was taken in to account when compiling the GRACE model, which has allowed for a reliable computation of the aforementioned noise full covariance matrices. The coloured (frequency-dependent) noise characteristic of KBR data was taken in to account when compiling the model, which has allowed for a reliable computation of these noise and signal covariance matrices. They play a crucial role when filtering and allow to achieve a higher spatial resolution compared to commonly applied GRACE filtering methods such as Gaussian smoothing and/or destriping filters. GRACE data are available for the period 01 January 2003 to 15 July 2016.

### 3.3 Model Outputs

To establish the quality of the STREAM v1.3 model in runoff simulation, monthly runoff ( $R$ ) data obtained from the Global Runoff Reconstruction (GRUN\_v1, <https://doi.org/10.3929/ethz-b-000324386>) have been used for comparison. The GRUN dataset (Ghiggi et al., 2019) is a global monthly  $R$  dataset derived through the use of a machine learning algorithm trained with in situ  $Q$  observations of relatively small catchments (<2500 km<sup>2</sup>) and gridded precipitation and temperature

247 derived from the Global Soil Wetness Project Phase 3 (GSWP3) dataset ([Kim et al., 2017](#)). The  
248 dataset covers the period from 1902 to 2014 and it is provided on a  $0.5^\circ \times 0.5^\circ$  regular grid.

## 249 **4. METHOD**

### 250 **4.1 STREAM Model: the Concept**

251 The concept behind the STREAM v1.3 model is that river discharge is a combination of hydrological  
252 responses operating at diverse time scales ([Blöschl et al., 2013](#); [Rakovec et al., 2016](#)). In particular,  
253 river discharge can be considered made up of a *slow-flow component*, produced as outflow of the  
254 groundwater storage and of a *quick-flow component*, i.e. mainly related to the surface and subsurface  
255 runoff components ([Hu and Li, 2018](#)).

256 While the high spatial and temporal (i.e., intermittence) variability of precipitation and the highly  
257 changing land cover spatial distribution significantly impact the variability of the *quick-flow*  
258 *component* (with scales ranging from hours to days and meters to kilometres depending on the basin  
259 size), *slow-flow river discharge* reacts to precipitation inputs more slowly (i.e., months) as water  
260 infiltrates, is stored, mixed and is eventually released in times spanning from weeks to months.  
261 Therefore, the two components can be estimated by relying upon two different approaches that  
262 involve different types of observations. Based on that, within the STREAM v1.3 model, satellite soil  
263 moisture, precipitation and TWSA will be used for deriving river discharge and runoff estimates. The  
264 first two variables are used as proxy of the *quick-flow* river discharge component while TWSA is  
265 exploited for obtaining its complementary part, i.e., the *slow-flow river discharge* component. Firstly,  
266 we exploit the role of the soil moisture in determining the response of the catchment to the  
267 precipitation inputs, which have been soundly demonstrated in more than ten years of literature  
268 studies (see e.g., [Brocca et al., 2017](#) for a comprehensive discussion on the topic). Secondly, we  
269 consider the important role of terrestrial water storage in determining the slow-flow river discharge  
270 component as modelled in several hydrological models (e.g., [Sneeuw et al., 2014](#)).

271 It is worth noting that this *modus operandi*, i.e. to model the *quick-flow* and *slow-flow* discharge  
272 component separately exploring their process controls independently, has been largely applied and  
273 tested in recent and past studies, e.g., for the estimation of the flow duration curve (see e.g. Botter et  
274 al., 2007a, b; Yokoo and Sivapalan 2011; Muneepeerakul et al., 2010; Ghotbi et al., 2020).

#### 275 **4.2 STREAM Model: the Laws**

276 The STREAM v1.3 model is a conceptual hydrological model that, by using as input observation of  
277  $P$ , soil moisture, TWSA and  $T_{\text{air}}$  data, simulates continuous  $R$  and  $Q$  time series.

278 The model entails three main components (Figure 1): 1) a snow module to separate precipitation into  
279 snowfall and rainfall, 2) a soil module to simulate the evolution in time  $t$  of the quick and slow runoff  
280 responses,  $Q_{fu}$  [mm] and  $Q_{sl}$  [mm], and 3) a routing module that transfers these components through  
281 the basins and the rivers for the simulation of the *quick-flow* river discharge,  $QF$  [m<sup>3</sup>/s], and the *slow-*  
282 *flow* river discharge,  $SF$  [m<sup>3</sup>/s] components.

283 The soil module is composed of two storages,  $S_u$  and  $S_l$  as illustrated in Figure 1. The upper storage  
284 receives inputs from  $P$ , released through a snow module (Cislaghi et al., 2020) as rainfall ( $r$ ) or stored  
285 as snow water equivalent ( $SWE$ ) within the snowpack and on the glaciers. In particular, according to  
286 Cislaghi et al. (2020),  $SWE$  is modelled by using as input  $T_{\text{air}}$  and a degree-day coefficient,  $C_m$ , to be  
287 estimated by calibration.

288 Once separated,  $r$  input contributes to the quick runoff response while the  $SWE$  (like other fluxes  
289 contributing to modify the soil water content into  $S_u$ ) is neglected as already considered in the satellite  
290 TWSA. Therefore, the first key point of the STREAM v1.3 model is that the water content in the  
291 upper storage is directly provided by the satellite soil moisture observations and the loss processes  
292 like infiltration or evaporation do not need to be explicitly modelled to simulate the evolution in time  
293  $t$  of soil moisture. Consequently, the quick runoff response,  $Q_{fu}$  from the first storage can be  
294 computed following the formulation proposed by Georgakakos and Baumer (1996), as in equation  
295 (1):

$$Qfu(t) = r(t) SWI(t, T)^\alpha \quad (1)$$

where:

-  $SWI$  is the Soil Water Index (Wagner et al., 1999), i.e., the root-zone soil moisture product referred to the first layer of the model (representative of the first 5-30 centimeters of soil), derived by the surface satellite soil moisture product,  $\theta$ , by applying the exponential filtering approach in its recursive formulation (Albergel et al., 2009):

$$SWI_n = SWI_{n-1} + K_n(\theta(t_n) - SWI_{n-1}) \quad (2)$$

with the gain  $K_n$  at the time  $t_n$  given by:

$$K_n = \frac{K_{n-1}}{K_{n-1} + e^{\left(\frac{t_n - t_{n-1}}{T}\right)}} \quad (3)$$

- $T$  [days] is a parameter, named characteristic time length, that characterizes the temporal variation of soil moisture within the root-zone profile and the gain  $K_n$  ranges between 0 and 1;
- $\alpha$  [-] is a coefficient linked to the non-linearity of the infiltration process and it takes into account the characteristics of the soil;
- for the initialization of the filter  $K_1 = 1$  and  $SWI_1 = \theta(t_1)$ .

The second key point of STREAM v1.3 model concerns the estimation of the slow runoff response,  $Qsl$ , from the second storage. The hypothesis here, shared also with other studies (e.g., Rakovec et al., 2016), is that the dynamic of the slow runoff component can be represented by the monthly TWSA data. Indeed, the time scale of slow runoff response is typically in the range of seasons to years and it can be assumed almost independent upon the water that is contained in that upper storage. For that, the slow runoff response  $Qsl$ , from the second storage, can be computed following the formulation proposed by Famiglietti and Wood (1994), through equation (4) as follows:

$$Qsl(t) = \beta (TWSA^*(t))^m \quad (4)$$

where:

319 -  $TWSA^*$  [-] is the TWSA estimated by GRACE normalized by its minimum and maximum values.

320 The assumption behind this equation is that TWSA can be assumed as a proxy of the evolution in

321 time,  $t$ , of the  $Sl$ , i.e., the storage of the lower storage.

322 -  $\beta$  [mm h<sup>-1</sup>] and  $m$  [-] are two parameters describing the nonlinearity between slow runoff

323 component and  $TWSA^*$ .

324 Note that we made the hypothesis that soil moisture and TWSA observations are independent

325 (whereas in the reality soil moisture can be responsible both for the generation of the quick flow part

326 (mainly) and for the slow flow contribution) given the different temporal (and spatial) scales at which

327 the quick and slow runoff responses act.

328 The STREAM v1.3 model runs in a semi-distributed version in which the catchment is divided into

329  $s$  elements, each one representing either a subcatchment with outlet along the main channel or an area

330 draining directly into the main channel. Each element is assumed homogeneous and hence constitutes

331 a lumped system.

332 The routing module (controlled by a  $\gamma$  parameter) conveys the  $Qfu$  and  $Qsl$  response components at

333 each element outlet (subcatchments and directly draining areas, Brocca et al., 2011) and successively

334 at the catchment outlet of the basin. Specifically, the quick component  $Qfu$  is routed to the element

335 outlet by the Geomorphological Instantaneous Unit Hydro-graph (GIUH, Gupta et al., 1980) for

336 subcatchments or through a linear reservoir approach (Nash, 1957) for directly draining areas; the

337  $Qsl$  slow component is transferred to the outlet section by a linear reservoir approach. Finally, a

338 diffusive linear approach (controlled by the parameters  $C$  and  $D$ , i.e., Celerity and Diffusivity,

339 Troutman and Karlinger, 1985) is applied to route the quick and slow runoff components at the outlet

340 section of the catchment (Brocca et al., 2011). In the first case we obtain the *quick-flow* river discharge

341 component,  $QF$  [m<sup>3</sup>/s], and in the second case the *slow-flow* river discharge component,  $SF$  [m<sup>3</sup>/s]

342 (see Figure 1).

### 4.3 STREAM Parameters

The STREAM v1.3 model uses 8 parameters of which 5 are used in the soil module ( $\alpha$ ,  $T$  [days],  $\beta$  [mm h<sup>-1</sup>],  $m$ ,  $C_m$ ) and 3 in the routing module ( $\gamma$ ,  $C$  [km h<sup>-1</sup>] and  $D$  [km<sup>2</sup> h<sup>-1</sup>]). The parameter values, determined within the feasible parameter space (See Table Appendix A for more details), are calibrated by maximizing the Kling-Gupta Efficiency index (KGE, Gupta et al., 2009; Kling et al., 2012, see paragraph 5.1 for more details) between observed and simulated river discharge.

## 5. EXPERIMENTAL DESIGN

### 5.1 Modelling Setup for Mississippi River Basin

The modelling setup is carried out in four steps (Figure 2):

1. *Input data collection.* Two different groups of data have to be collected to setup the model, i.e., topographic information and hydrological variables. Concerning the topographic information, the SHuttle Elevation Derivatives at multiple Scales (HydroSHED, <https://www.hydrosheds.org/>) DEM of the basin at the 3'' resolution (nearly 90 m at the equator) as well as the location of the gauging stations where the model should be calibrated/validated, are collected. Concerning the hydrological variables, gridded precipitation,  $T_{air}$ , soil moisture and TWSA are collected. In addition, in situ  $Q$  time series for the sections where the model should be calibrated/validated as well as modelled runoff datasets are required.

2. *Sub-basin delineation.* STREAM v1.3 model is run in the semi-distributed version over the Mississippi River basin. The TopoToolbox (<https://topotoolbox.wordpress.com/>), a tool developed in Matlab by Schwanghart et al. (2010), and the DEM of the basin have been used to derive flow directions, to extract the stream network and to delineate the drainage basins over the Mississippi River basin. In particular, by considering only rivers with order greater than 3 (according to the Horton-Strahler rules, Horton, 1945; Strahler, 1952), the Mississippi watershed has been divided into

366 53 sub-basins as illustrated in Figure 3. Red dots in the figure indicate the location of the 11 discharge  
367 gauging stations selected for the study area.

368 It has to be specified that the step of sub-basin delineation could be accomplished through tools  
369 different from the TopoToolbox. For instance, it could be used the free Qgis software downloadable  
370 at <https://www.qgis.org/it/site/forusers/download.html>, following the instruction to perform the  
371 hydrological analysis as in  
372 [https://docs.qgis.org/3.16/en/docs/training\\_manual/processing/hydro.html?highlight=hydrological%](https://docs.qgis.org/3.16/en/docs/training_manual/processing/hydro.html?highlight=hydrological%20analysis)  
373 [20analysis](https://docs.qgis.org/3.16/en/docs/training_manual/processing/hydro.html?highlight=hydrological%20analysis).

374 3. *Extraction of input data.* Precipitation,  $T_{air}$ , soil moisture and TWSA datasets data have to be  
375 extracted for each sub-basin of the study area. If characterized by different spatial/temporal  
376 resolution, these datasets need to be resampled over a common spatial grid/temporal time step prior  
377 to be used as input into the model.

378 To run the STREAM v1.3 model over the Mississippi river basin, input data have been resampled  
379 over the precipitation spatial grid at  $0.25^\circ$  resolution through a bilinear interpolation. Concerning the  
380 temporal scale,  $T_{air}$ , soil moisture and precipitation data are available at daily time step, while monthly  
381 TWSA data have been linearly interpolated at daily time step. For each of the 53 Mississippi  
382 subbasins, the resampled precipitation, soil moisture,  $T_{air}$  and TWSA data have been extracted.

383 4. *STREAM model calibration.* In situ river discharge data are used as reference data for the  
384 calibration of STREAM v1.3 model. For Mississippi, the STREAM v1.3 model has been calibrated  
385 over five sections as illustrated in Figure 3: the inner sections 4, 6, 9, 11 and the outlet section 10, are  
386 used to calibrate the model and all sub-basins contributing to the respective sections are highlighted  
387 with the same colour. This means that, for example, the sub-basins labelled as 1, 2, 5 to 15, 17, 22,  
388 23, and 30 contribute to section 4, sub-basins 31, 37, 38 and 41 contribute to section 6 and so on.  
389 Consequently, the sub-basins highlighted with the same colour are assigned the same model  
390 parameters, i.e. the parameters that allow to reproduce the river discharge data observed at the related  
391 outlet section.



392 Once calibrated, the STREAM v1.3 model has been run to provide continuous daily Q and R time  
393 series, at the outlet section of each subbasin and over each grid pixel, respectively. By considering  
394 the spatial/temporal availability of both in situ and satellite observations, the entire analysis period  
395 covers the maximum common observation period, i.e., from 01 January 2003 to 15 July 2016 at daily  
396 time scale. To establish the goodness-of-fit of the model, the simulated river discharge and runoff  
397 timeseries are compared against in situ river discharge and modelled runoff data.

## 398 **5.2 Model Evaluation Criteria and Performance Metrics**

399 The model has been run over a 13.5-year period split into two sub periods: the first 8 years, from  
400 January 2003 to December 2010, have been used to calibrate the model successively validated over  
401 the remaining 5.5 years (January 2011 - July 2016).

402 In particular, three different validation schemes have been adopted to assess the robustness of the  
403 STREAM v1.3 model:

- 404 1. Internal validation aimed to test the plausibility of both the model structure and the parameter  
405 set in providing reliable estimates of the hydrological variables against which the model is  
406 calibrated. For this purpose, a comparison between observed and simulated river discharge  
407 time series on the sections used for model calibration has been carried out for both the  
408 calibration and validation sub periods.
- 409 2. Cross-validation testing the goodness of the model structure and the calibrated model  
410 parameters to predict hydrological variables at locations not considered in the calibration  
411 phase. In this respect, the cross-validation has been carried out by comparing observed and  
412 simulated river discharge time series in gauged basins not considered during the calibration  
413 phase;
- 414 3. External validation aimed to test the capability of the model “*to get the right answers for the*  
415 *right reasons*” (Kirchner 2006). In this respect, the capability of the model to reproduce  
416 variables (e.g., fluxes or state variables) other than discharge and not considered in the  
417 calibration phase, should be tested. As runoff is a secondary product of the STREAM v1.3

model, obtained indirectly from the calibration of the river discharge (basin-integrated runoff), the comparison in terms of runoff can be considered as a further external validation of the model. Runoff, differently from discharge, cannot be directly measured. It is generally modelled through land surface or hydrological models. Its validation requires a comparison against modelled data that, however, suffer from uncertainties (Beck et al., 2017). Based on that, in this study the GRUN runoff dataset described in the section 3.3 has been used for a qualitative comparison.

### 5.3 Performance Metrics

To measure the goodness-of-fit between simulated and observed river discharge data three performance scores have been used:

- the relative root mean square error, RRMSE:

$$RRMSE = \frac{\sqrt{\frac{1}{n} \sum_{i=1}^n (Q_{sim_i} - Q_{obs_i})^2}}{\frac{1}{n} \sum_{i=1}^n (Q_{obs_i})} \quad (5)$$

where  $Q_{obs}$  and  $Q_{sim}$  are the observed and simulated discharge time series of length  $n$ . RRMSE values range from 0 to  $+\infty$ , the lower the RRMSE, the better the agreement between observed and simulated data.

- the Pearson correlation coefficient,  $R$ , measures the linear relationship between two variables:

$$R = \frac{\sum_{i=1}^n (Q_{sim_i} - \overline{Q_{sim}})(Q_{obs_i} - \overline{Q_{obs}})}{\sqrt{\sum_{i=1}^n (Q_{sim_i} - \overline{Q_{sim}})^2 (Q_{obs_i} - \overline{Q_{obs}})^2}} \quad (6)$$

where  $\overline{Q_{obs}}$  and  $\overline{Q_{sim}}$  represent the mean values of  $Q_{obs}$  and  $Q_{sim}$ , respectively. The values of  $R$  range between  $-1$  and  $1$ ; higher values of  $R$  indicate a better agreement between observed and simulated data.

- the Kling-Gupta efficiency index (KGE, Gupta et al., 2009), which provides direct assessment of four aspects of discharge time series, namely shape, timing, water balance and variability. It is defined as follows:

$$KGE = 1 - \sqrt{(R - 1)^2 + (\delta - 1)^2 + (\varepsilon - 1)^2} \quad (7)$$

442 where  $R$  is the correlation coefficient,  $\delta$  the relative variability and  $\varepsilon$  the bias normalized by the  
443 standard deviation between observed and simulated discharge. The KGE values range between  $-\infty$   
444 and 1; the higher the KGE, the better the agreement between observed and simulated data.  
445 Simulations characterized by values of KGE in the range -0.41 and 1 can be assumed as reliable;  
446 values of KGE greater than 0.5 have been assumed good with respect to their ability to reproduce  
447 observed time series (Thiemig et al., 2013).

## 448 **6. RESULTS**

449 The testing and validation of the STREAM v1.3 model is presented and discussed in this section  
450 according to the scheme illustrated in section 5.2.

### 451 **6.1 Internal Validation**

452 The performance of the STREAM v1.3 model over the calibrated river sections is illustrated in Figure  
453 4 and summarized in Table 2. Figure 4 shows observed and simulated river discharge time series over  
454 the whole study period (2003-2016); in Table 2 the performance scores are evaluated separately for  
455 the calibration and validation sub periods. It is worth noting that the model accurately simulates the  
456 observed river discharge data and is able to give the “right answer” with good modelling  
457 performances. Score values of KGE and  $R$  over the calibration (validation) period are higher than  
458 0.62 (0.67) and 0.75 (0.75) (resp.) for all the sections; RRMSE is lower than 46% (51%) for all the  
459 sections except for section 9, where it rises up to 71% (77%). The performances remain good even if  
460 they are evaluated over the entire study period as indicated by the scores on the top of each plot of  
461 Figure 4.

### 462 **6.2 Cross-validation**

463 The cross-validation has been carried out over the six river sections illustrated in Figure 5 not used  
464 in the calibration step. The performance scores on the top of each plot refer to the entire study periods;  
465 the scores split for calibration and validation periods are reported in Table 2. For some river sections  
466 the performance is quite low (see, e.g., river section 1, 2 and 5) whereas for others the model is able

to simulate the observed discharge data quite accurately (e.g., 7 and 8). In particular, for river sections 1 and 2 even if KGE reaches values equal to 0.35 and 0.40 (for the whole period), respectively, there is not a good agreement between observed and simulated river discharge and the R score is lower than 0.55 for both river sections. The worst performance is obtained over section 5, with negative KGE and low R (high RRSME). These results are certainly influenced by the presence of large dams located upstream to these river sections (i.e., Garrison, Gavins Point and Kanopolis dams, see Table 1) which have a strong impact on discharge: the model, not having a specific module for modelling reservoirs, is not able to accurately reproduce the dynamics of river discharge over regulated river sections. Positive KGE values are obtained over river sections 3, 7 and 8. In particular, over section 3 the STREAM v1.3 model overestimates the observed river discharge due the presence of large dams along the Missouri river. Over section 7, located over the Rock river, a relatively small tributary of Mississippi river (see Table 1), the STREAM v1.3 model overestimation has to be attributed to: 1) the different characteristics of the Rock river basin with respect to the entire basin closed to section 6 where the model has been calibrated (see Figure 3); 2) the small size of the Rock river basin (23'000 km<sup>2</sup>, if compared with GRACE resolution, 160'000 km<sup>2</sup>) for which the model accuracy is expect to be lower. Conversely, the performances over river section 8, whose parameters have been set equal to the ones of river section 10, are quite high (KGE equal to 0.71, 0.80 and 0.77 for the entire, the calibration and the validation period, respectively; R equal to 0.83, 0.84 and 0.84 for the entire, calibration and validation periods, respectively).

Although it is expected that the performances of STREAM v1.3 model, as any hydrological model calibrated against observed data, can decrease over the gauging sections not used for the calibration, the findings obtained above raises doubts about the robustness of model parameters and whether it is actually possible to transfer model parameters from one river section to another with different interbasin characteristics. A more in-depth investigation about the model calibration procedure, with special focus on the regionalization of the model parameters, should be carried out but this topic is beyond the scope of the manuscript.

### 493    **6.3 External Validation**

494    For the external validation, the monthly runoff time series provided by the GRUN datasets have been  
495    compared against the ones computed by the STREAM v1.3 model. For that, STREAM daily runoff  
496    time series have been aggregated at monthly scale and re-gridded at the same spatial resolution of the  
497    GRUN dataset (0.5°). The comparison is illustrated in Figure 6 for the common period 2003–2014.  
498    Although the two datasets consider different precipitation inputs, the two models agree in identifying  
499    two distinct zones in terms of runoff, i.e., the western dry and the eastern wet area. This two distinct  
500    zones can be clearly identified also in the GSWP3 and TMPA 3B42 V7 precipitation maps (not shown  
501    here) used as input in GRUN and STREAM v1.3, respectively, stressing that STREAM runoff output  
502    is correctly driven by the input data. However, likely due to the calibration procedure, the STREAM  
503    runoff map appears patchier with respect to GRUN and discontinuities along the sub-basin boundaries  
504    (identified in Figure 3) can be noted. This should be ascribed to the automatic calibration procedure  
505    of the model that, differently from other calibration techniques (e. g., regionalization procedures),  
506    does not consider the basin physical attributes like soil, vegetation, and geological properties that  
507    govern spatial dynamics of hydrological processes. This calibration procedure can generate sharp  
508    discontinuities even for neighbouring subcatchments individually calibrated. It leads to  
509    discontinuities in model parameter values and consequently in the simulated hydrological variable  
510    (runoff).

## 511    **7. DISCUSSION**

512    In the previous sections, the ability of the STREAM v1.3 model to accurately simulate river discharge  
513    and runoff time series has been presented. In particular, Figures 4, 5 and 6 demonstrate that satellite  
514    observations of precipitation, soil moisture and terrestrial water storage anomalies can provide  
515    accurate daily river discharge estimates for near-natural large basins (absence of upstream dams), and  
516    for basins with draining area lower than 160'000 km<sup>2</sup> (see section 7), i.e., at spatial/temporal  
517    resolution lower than the ones of the TWSA input data (monthly, 160'000 km<sup>2</sup>). This is an important

518 result of the study as it demonstrates, on one hand, that the model structure is appropriate with respect  
519 to the data used as input and, on the other hand, the great value of information contained into TWSA  
520 data that, even if characterized by limited spatial/temporal resolution, can be used to simulate runoff  
521 and river discharge at basin scale. This finding has been also confirmed by a preliminary sensitivity  
522 analysis in which the STREAM v1.3 model has been run with different hydrological inputs of  
523 precipitation, soil moisture and total water storage anomaly (not shown here for brevity). In particular,  
524 by running the STREAM v1.3 model with different input configurations (e.g., by using TMPA 3B42  
525 V7 or Climate Prediction Center (CPC) data for precipitation, ESA CCI or Advanced SCATterometer  
526 (ASCAT) data for soil moisture, TWSA or soil moisture data to simulate the slow-flow river  
527 discharge component), we found that STREAM results are more sensitive to soil moisture data rather  
528 than to precipitation input. In addition, by running STREAM v1.3 model with soil moisture data as  
529 input to simulate the slow-flow river discharge component (i.e. without using TWSA data) we found  
530 a deterioration of the model results.

531 Hereinafter, the strengths and the main limitations of the STREAM v1.3 model are discussed.

532 Among the strengths of the STREAM v1.3 model it is worth highlighting:

533 **1. Remote sensing-based conceptual hydrological model.** Discharge and runoff estimates are  
534 obtained through a remote sensing-based conceptual hydrological model, simpler than classical  
535 hydrological models or LSMs. In particular, discharge and runoff estimates are obtained by exploiting  
536 as much as possible satellite observations and by keeping the modelling component at a minimum.  
537 The knowledge of the key mechanisms and processes that act in the formation of runoff, like the role  
538 of the soil moisture in determining the response of the catchment to precipitation, played a major role  
539 in the definition of the model structure. Being an observational-based approach, the STREAM v1.3  
540 model presents two main advantages: 1) possibility to directly ingest observations (soil moisture and  
541 terrestrial water storage data) into the model structure, allowing to take implicitly into account some  
542 processes, mainly human-driven (e.g., irrigation, change in the land use), which might have a large  
543 impact on the hydrological cycle and hence on total runoff; 2) the independence with respect to

544 existing large scale hydrological models such as, e.g., the evapotranspiration is not explicitly  
545 modelled.

546 2. **Simplicity.** The STREAM v1.3 model structure: 1) limits the input data required (only  
547 precipitation,  $T_{\text{air}}$ , soil moisture and TWSA data are needed as input; LSM/GHMs require many  
548 additional inputs such as wind speed, shortwave and longwave radiation, pressure and relative  
549 humidity); 2) limits and simplifies the processes to be modelled for runoff/discharge simulation.  
550 Processes like evapotranspiration, infiltration or percolation, are not modelled therefore avoiding the  
551 need of using sophisticated and highly parameterized equations (e.g., Penman-Monteith for  
552 evapotranspiration, Allen et al.,1998, Richard equation for infiltration, Richard, 1931); 3) limits the  
553 number of parameters (only 8 parameters have to be calibrated) thus simplifying the calibration  
554 procedure and potentially reduce the model uncertainties related to the estimation of parameter  
555 values.

556 3. **Versatility.** The STREAM v1.3 model is a versatile model suitable for daily runoff and discharge  
557 estimation over sub-basins with different physiographic characteristics. The results obtained in this  
558 study clearly indicate the potential of this approach to be extended at the global scale. Moreover, the  
559 model can be easily adapted to ingest input data with spatial/temporal resolution different from the  
560 one tested in this study (0.25°/daily). For instance, satellite missions with higher space/time  
561 resolution, or near real time satellite products could be considered. As an example, the Next  
562 Generation Gravity Mission design studies all encompass double-pair scenarios, which would greatly  
563 improve upon the current spatial resolution of single-pair missions like GRACE and GRACE-FO (>  
564 100'000 km<sup>2</sup>).

565 4. **Computationally inexpensive.** Due to its simplicity and the limited number of parameters to be  
566 calibrated, the computational effort for the STREAM v1.3 model is very limited.

567

568 However, some limitations have to be acknowledged for the current version of the STREAM v1.3  
569 model:

570 **1. Presence of reservoir, diversion, dams or flood plain.** As the STREAM v1.3 model does not  
571 explicitly consider the presence of discontinuity elements along the river network (e. g, reservoir,  
572 dam or floodplain), discharge estimates obtained for sections located downstream of such elements  
573 might be inaccurate (see, e.g., river sections 1 and 2 in Figure 5).

574 **2. Need of in situ data for model calibration and robustness of model parameters.** As discussed  
575 in the results section, parameter values of the STREAM v1.3 model are set through an automatic  
576 calibration procedure aimed at minimizing the differences between simulated and observed river  
577 discharge. The main drawback of this parameterization technique is that the models parameterized  
578 with this technique may exhibit (1) poor predictability of state variables and fluxes at locations and  
579 periods not considered in the calibration, and (2) sharp discontinuities along sub-basin boundaries in  
580 state flux, and parameter fields (e.g., Merz and Blöschl, 2004).

581 To overcome these issues, several regionalization procedures, as for instance summarized in Cislaghi  
582 et al. (2020), could be conveniently applied to transfer model parameters from hydrologically similar  
583 catchments to a catchment of interest. In particular, the regionalization of model parameters could  
584 allow to: i) estimate discharge and runoff time series over ungauged basins overcoming the need of  
585 discharge data recorded from in-situ networks; ii) estimate the model parameter values through a  
586 physically consistent approach, linking them to the characteristics of the basins; iii) solve the problem  
587 of discontinuities in the model parameters, avoiding to obtain patchy unrealistic runoff maps. As this  
588 aspect requires additional investigations and it is beyond the paper purpose, it will not be tackled  
589 here.

## 590 **8. CONCLUSIONS**

591 This study presents a new conceptual hydrological model, STREAM v1.3, for runoff and river  
592 discharge estimation. By using as input satellite data of precipitation, soil moisture and terrestrial



593 water storage anomalies, the model has been able to provide accurate daily river discharge and runoff  
594 estimates at the outlet river section and the inner river sections and over a  $0.25^{\circ} \times 0.25^{\circ}$  spatial grid of  
595 the Mississippi river basin. In particular, the model is suitable to reproduce:

- 596 1. river discharge time series over the calibrated river section with good performances both in  
597 calibration and validation periods;
- 598 2. river discharge time series over river sections not used for calibration and not located downstream  
599 dams or reservoirs;
- 600 3. runoff time series with a quite good agreement with respect to the well-established GRUN  
601 observational-based dataset used for comparison.

602 The integration of observations of soil moisture, precipitation and terrestrial water storage anomalies  
603 is a first alternative method for river discharge and runoff estimation with respect to classical methods  
604 based on the use of TWSA-only (suitable for river basins larger than  $160'000 \text{ km}^2$ , monthly time  
605 scale) or on classical LSMs ([Cai et al., 2014](#)).

606 Moreover, although simple, the model has demonstrated a great potential to be easily applied over  
607 subbasins with different climatic and topographic characteristics, suggesting also the possibility to  
608 extend its application to other basins. In particular, the analysis over basins with high human impact,  
609 where the knowledge of the hydrological cycle and the river discharge monitoring is very important,  
610 deserves special attention. Indeed, as the STREAM v1.3 model is directly ingesting observations of  
611 soil moisture and terrestrial water storage data, it allows the modeller to neglect processes that are  
612 implicitly accounted for in the input data. Therefore, human-driven processes (e.g., irrigation, land  
613 use change), that are typically very difficult to simulate due to missing information and might have a  
614 large impact on the hydrological cycle, hence on total runoff, could be implicitly modelled. The  
615 application of the STREAM v1.3 model on a larger number of basins with different climatic-  
616 physiographic characteristics (e.g., including more arid basins, snow-dominated, lots of topography,  
617 heavily managed) will allow to investigate the possibility to regionalize the model parameters and  
618 overcome the limitations of the automatic calibration procedure highlighted in the discussion section.

## 619 **AUTHOR CONTRIBUTION**

620 S.C. performed the analysis and wrote the manuscript. G.G. collected the data and helped in  
621 performing the analysis; C.M, L.B., A.T., N.S., H.H.F., C.M., M.R. and J.B. contributed to the  
622 supervision of the work. All authors discussed the results and contributed to the final manuscript.

## 623 **CODE AVAILABILITY**

624 The STREAM model version 1.3, with a short user manual, is freely downloadable in Zenodo  
625 (<https://zenodo.org/record/4744984>, doi: 10.5281/zenodo.4744984). The STREAM v1.3 model code  
626 is distributed through M language files, but it could be run with different interpreters of M language,  
627 like the GNU Octave (freely downloadable here <https://www.gnu.org/software/octave/download>).

## 628 **DATA AVAILABILITY**

629 All data and codes used in the study are freely available online. Air temperature data are available at  
630 <https://psl.noaa.gov/data/gridded/data.cpc.globaltemp.html> (last access 25/11/202). In situ river  
631 discharge data have been taken from the Global Runoff Data Center (GRDC,  
632 [https://www.bafg.de/GRDC/EN/Home/homepage\\_node.html](https://www.bafg.de/GRDC/EN/Home/homepage_node.html) (last access 25/11/202). Precipitation  
633 and soil moisture data are available from <http://pmm.nasa.gov/data-access/downloads/trmm> and  
634 <https://esa-soilmoisture-cci.org/>, respectively.

## 635 **COMPETING INTERESTS**

636 The authors declare that they have no conflict of interest.

## 637 **ACKNOWLEDGMENTS**

638 The authors wish to thank the Global Runoff Data Centre (GRDC) for providing most of the  
639 streamflow data throughout Europe. The authors gratefully acknowledge support from ESA through

640 the STREAM Project (EO Science for Society element Permanent Open Call contract n°  
641 4000126745/19/I-NB).  
642

## 643 REFERENCE

- 644 Albergel, C., Rüdiger, C., Carrer, D., Calvet, J. C., Fritz, N., Naeimi, V., Bartalis, Z., and Hasenauer, S. (2009).: An  
645 evaluation of ASCAT surface soil moisture products with in-situ observations in southwestern France. , Hydrol. Earth  
646 Syst. Sci. Hydrology and Earth System Sciences, 13, 115–124, <https://doi.org/doi:10.5194/hess-13-115-2009>, 2009..
- 647 Alexander, J. S., Wilson, R. C., and Green, W. R.: A brief history and summary of the effects of river engineering and  
648 dams on the Mississippi River system and delta (p. 53), US Department of the Interior, US Geological Survey,  
649 <https://doi.org/10.3133/cir1375>, 2012.
- 650 Allen, R.G., Pereira, L. S., Raes, D., and Smith, M: Crop evapotranspiration — guidelines for computing crop water  
651 requirements. FAO Irrigation & Drainage Paper 56. FAO, Rome, 1988.
- 652 Balsamo, G., A. Beljaars, K. Scipal, P. Viterbo, B. vanden Hurk, M. Hirschi, and A. K. Betts: A revised hydrology for  
653 the ECMWF model: Verification from field site to terrestrial water storage and impact in the integrated forecast  
654 system, J. Hydrometeorol., 10(3), 623–643, <https://doi.org/doi:10.1175/2008JHM1068.1>, 2009.
- 655 Barbarossa, V., Huijbregts, M. A., Beusen, A. H., Beck, H. E., King, H., and Schipper, A. M.: FLO1K, global maps of  
656 mean, maximum and minimum annual streamflow at 1 km resolution from 1960 through 2015, Scientific Sci. Data,  
657 55, 180052, <https://doi.org/10.1038/sdata.2018.52>, 2018.
- 658 Beck, H. E., van Dijk, A. I., de Roo, A., Dutra, E., Fink, G., Orth, R., and Schellekens, J.: Global evaluation of runoff  
659 from ten state-of-the-art hydrological models, Hydrol. Earth Syst. Sci., 21(6), 2881-2903. <https://doi.org/doi:10.5194/hess-21-2881-2017>, 2017.
- 660 Berghuijs, W. R., Woods, R. A., Hutton, C. J., and Sivapalan, M.: Dominant flood generating mechanisms across the  
661 United States, Geophys. Res. Lett., 43, 4382–4390, <https://doi.org/10.1002/2016GL068070>, 2016.
- 662 Berthet, L., Andréassian, V., Perrin, C., and Javelle, P.: How crucial is it to account for the antecedent moisture conditions  
663 in flood forecasting? Comparison of event-based and continuous approaches on 178 catchments, Hydrol. Earth Syst.  
664 Sci., 13(6), 819-831, 2009.
- 665 Blöschl, G., Sivapalan, M., Wagener, T., Viglione, A., and Savenije, H. H. G. (Eds.): Runoff predictions in ungauged  
666 basins: A synthesis across processes, places and scales, Cambridge: Cambridge University Press, 2013.
- 667 Botter, G., Porporato, A., Daly, E., Rodriguez-Iturbe, I., and Rinaldo, A.: Probabilistic characterization of base flows in  
668 river basins: Roles of soil, vegetation, and geomorphology, Water Resour. Res., 43, W06404,  
669 <https://doi.org/doi:10.1029/2006WR005397>, 2007a.
- 670 Botter, G., Peratoner, F., Porporato, A., Rodriguez-Iturbe, I., and Rinaldo, A.: Signatures of large-scale soil moisture  
671 dynamics on streamflow statistics across U.S. Climate regimes, Water Resour. Res., 43, W11413,  
672 <https://doi.org/doi:10.1029/2007WR006162>, 2007b.
- 673 Brocca, L., Ciabatta, L., Massari, C., Camici, S., and Tarpanelli, A.: Soil moisture for hydrological applications: open  
674 questions and new opportunities, Water, 9(2), 140, <https://doi.org/10.3390/w9020140>, 2017.
- 675 Brocca, L., Melone, F., and Moramarco, T.: Distributed rainfall-runoff modelling for flood frequency estimation and  
676 flood forecasting, Hydrol. Process., 25(18), 2801-2813, <https://doi.org/10.1002/hyp.8042>, 2011.
- 677 Brocca, L., Melone, F., and Moramarco, T.: On the estimation of antecedent wetness conditions in rainfall-runoff  
678 modelling, Hydrol. Process., 22 (5), 629-642, doi:10.1002/hyp.6629. <https://doi.org/10.1002/hyp.6629>, 2008.
- 679 Brocca, L., Melone, F., Moramarco, T., and Morbidelli, R.: Antecedent wetness conditions based on ERS scatterometer  
680 data, J. Hydrol., 364(1-2), 73-87, <https://doi.org/10.1016/j.jhydrol.2008.10.007>, 2009.
- 681 Cai, X., Yang, Z. L., David, C. H., Niu, G. Y., and Rodell, M.: Hydrological evaluation of the Noah-MP land surface  
682 model for the Mississippi River Basin, J. Geophys. Res. Atmos., 119(1), 23-38,  
683 <https://doi.org/10.1002/2013JD020792>, 2014.
- 684 Cislighi, A., Masseroni, D., Massari, C., Camici, S., and Brocca, L.: Combining a rainfall–runoff model and a  
685 regionalization approach for flood and water resource assessment in the western Po Valley, Italy, Hydrol. Sci. J.,  
686 65(3), 348-370, <https://doi.org/10.1080/02626667.2019.1690656>, 2020.

688 Crochemore, L., Isberg, K., Pimentel, R., Pineda, L., Hasan, A., and Arheimer, B.: Lessons learnt from checking the  
689 quality of openly accessible river flow data worldwide, *Hydrol. Sci. J.*, 65(5), 699-711,  
690 <https://doi.org/10.1080/02626667.2019.1659509>, 2020.

691 Crow, W. T., Bindlish, R., and Jackson, T. J.: The added value of spaceborne passive microwave soil moisture retrievals  
692 for forecasting rainfall-runoff partitioning, *Geophys. Res. Lett.*, 32(18), <https://doi.org/10.1029/2005GL023543>,  
693 2005.

694 Döll, P., F.Kaspar, and B.Lehner: A global hydrological model for deriving water availability indicators: Model tuning  
695 and validation, *J. Hydrol.*, 270(1–2), 105–134, [https://doi.org/doi:10.1016/S0022-1694\(02\)00283-4](https://doi.org/doi:10.1016/S0022-1694(02)00283-4), 2003.

696 Dorigo, W., Wagner, W., Albergel, C., Albrecht, F., Balsamo, G., Brocca, L., Chung, D., Ertl, M., Forkel, M., Gruber, A.,  
697 Haas, D., Hamer, P., Hirschi, M., Ikonen, J., de Jeu, R., Kidd, R., Lahoz, W., Liu, Y.Y., Miralles, D., Mistelbauer, T.,  
698 Nicolai-Shaw, N., Parinussa, R., Pratola, C., Reimer, C., van der Schalie, R., Seneviratne, S.I., Smolander, T., and  
699 Lecomte, P.: ESA CCI Soil Moisture for improved Earth system understanding: state-of-the art and future directions.,  
700 *Remote Sens. Environ.*, 203, 185-215, <https://doi.org/10.1016/j.rse.2017.07.001>, 2017.

701 Dyer, J.: Snow depth and streamflow relationships in large North American watersheds, *J. Geophys. Res.*, 113, D18113,  
702 <https://doi.org/10.1029/2008JD010031>, 2008.

703 Entekhabi, D., Njoku, E. G., O'Neill, P. E., Kellogg, K. H., Crow, W. T., Edelstein, W. N., ... and Van Zyl, J.: The soil  
704 moisture active passive (SMAP) mission. *Proceedings of the Institute of Electrical and Electronics Engineers (IEEE)*,  
705 98(5), 704-716. <https://doi.org/doi: 10.1109/JPROC.2010.2043918>, 2010.

706 Famiglietti, J. S., and Rodell, M.: Water in the balance, *Science*, 340(6138), 1300-1301,  
707 <https://doi.org/10.1126/science.1236460>, 2013.

708 Famiglietti, J.S., and Wood, E. F.: Multiscale modeling of spatially variable water and energy balance processes, *Water*  
709 *Resour. Res.*, 30, 3061–3078, <https://doi.org/10.1029/94WR01498>, 1994.

710 Fan, Y. and Van den Dool, H. A: Global monthly land surface air temperature analysis for 1948–present, *J. Geophys.*  
711 *Res. Atmos.*, 113, D01103, <https://doi.org/10.1029/2007JD008470>, 2008.

712 Fekete, B. M., Looser, U., Pietroniro, A., and Robarts, R. D.: Rationale for monitoring discharge on the ground, *J.*  
713 *Hydrometeorol.*, 13, 1977–1986, <https://doi.org/10.1175/JHM-D-11-0126.1>, 2012.

714 Georgakakos KP, and Baumer OW.: Measurement and utilization of onsite soil moisture data, *J. Hydrol.*, 184: , 131–152,  
715 [https://doi.org/10.1016/0022-1694\(95\)02971-0](https://doi.org/10.1016/0022-1694(95)02971-0), 1996.

716 Ghiggi, G., Humphrey, V., Seneviratne, S. I., and Gudmundsson, L.: GRUN: an observation-based global gridded runoff  
717 dataset from 1902 to 2014, *Earth Syst. Sci. Data*, 11, 1655–1674 *Earth System Science Data*, 11(4), 1655-1674,  
718 <https://doi.org/10.5194/essd-11-1655-2019>, 2019.

719 Ghotbi, S., Wang, D., Singh, A., Blöschl, G., and Sivapalan, M.: A New Framework for Exploring Process Controls of  
720 Flow Duration Curves, *Water Resour. Res.* *Water Resources Research*, 56(1), <https://doi.org/e2019WR026083>, 2020.

721 Gudmundsson, L., Wagener, T., Tallaksen, L. M., and Engeland, K.: Evaluation of nine large-scale hydrological models  
722 with respect to the seasonal runoff climatology in Europe, *Water Resour. Res.*, 48(11),  
723 <https://doi.org/10.1029/2011WR010911>, 2012a.

724 Gudmundsson, L., Tallaksen, L. M., Stahl, K., Clark, D. B., Du-mont, E., Hagemann, S., Bertrand, N., Gerten, D., Heinke,  
725 J., Hanasaki, N., Voss, F., and Koirala, S.: Comparing Large-Scale Hydrological Model Simulations to Observed  
726 Runoff Percentiles in Europe, *J. Hydrometeorol.*, 13, 604–62, <https://doi.org/10.1175/JHM-D-11-083.1>, 2012b.

727 Gudmundsson, L., and Seneviratne, S. I.: Observation-based gridded runoff estimates for Europe (E-RUN version 1.1),  
728 *Earth Syst. Sci. Data*, 8, 279–295, <https://doi.org/10.5194/essd-8-279-2016>, 8(2), 279-295 2016, 2016.

729 Gupta VK, Waymire E, and Wang CT.: A representation of an instantaneous unit hydrograph from geomorphology, *Water*  
730 *Resour. Res.*, 16: 855–862, <https://doi.org/doi: 10.1029/WR016i005p00855>, 1980.

731 Gupta, H. V., Kling, H., Yilmaz, K. K., and Martinez, G. F.: Decomposition of the mean squared error and NSE  
732 performance criteria: Implications for improving hydrological modelling, *J. Hydrol.*, 377(1-2), 80-91,  
733 <https://doi.org/10.1016/j.jhydrol.2009.08.003>, 2009.

734 Haddeland, I., Heinke, J., Voß, F., Eisner, S., Chen, C., Hagemann, S., and Ludwig, F.: Effects of climate model radiation,  
735 humidity and wind estimates on hydrological simulations, *Hydrol. Earth Syst. Sci.*, 16(2), 305-318,  
736 <https://doi.org/10.5194/hess-16-305-2012>, 2012.

737 Hastie, T., Tibshirani, R., and Friedman, J. H.: *The Elements of Statistical Learning – Data Mining, Inference, and*  
738 *Prediction*, Second Edition, Springer Series in Statistics, Springer, New York, 2nd Edn., available at: [http://www-](http://www-stat.stanford.edu/~tibs/ElemStatLearn/)  
739 [stat.stanford.edu/~tibs/ElemStatLearn/](http://www-stat.stanford.edu/~tibs/ElemStatLearn/) (last access: 5 July 2016)., 2009.

740 Hong, Y., Adler, R. F., Hossain, F., Curtis, S., and Huffman, G. J.: A first approach to global runoff simulation using  
741 satellite rainfall estimation, *Water Resour. Res.*, 43(8), <https://doi.org/10.1029/2006WR005739>, 2007.

742 Horton, R. E.: Hydrological approach to quantitative morphology, *Geol. Soc. Am. Bull.*, 56, 275-370, 1945.

743 Houborg, R., Rodell, M., Li, B., Reichle, R., and Zaitchik, B. F.: Drought indicators based on model-assimilated Gravity  
744 Recovery and Climate Experiment (GRACE) terrestrial water storage observations, *Water Resour. Res.*, 48(7),  
745 <https://doi.org/10.1029/2011WR011291>, 2012.

746 Hu GR., and Li XY.: Subsurface Flow. In: Li X., Vereecken H. (eds) *Observation and Measurement. Ecohydrology.*  
747 Springer, Berlin, Heidelberg. [https://doi.org/10.1007/978-3-662-47871-4\\_9-1](https://doi.org/10.1007/978-3-662-47871-4_9-1), 2018.

748 Huffman, G. J., Adler, R. F., Bolvin, D. T., Gu, G. J., Nelkin, E. J., Bowman, K. P., Hong, Y., Stocker, E. F. and Wolff,  
749 D. B.: The TRMM Multisatellite Precipitation Analysis (TMPA): Quasi-Global, Multiyear, Combined-Sensor  
750 Precipitation Estimates at Fine Scales, *J. Hydrometeorol.*, 8 (1): 38–55. <https://doi.org/doi:10.1175/jhm560.1>, 2007.

751 Huffman, G. J., Stocker, E. F., Bolvin, D. T., Nelkin, E. J., and Adler, R. F.: TRMM Version 7 3B42 and 3B43 Data Sets.  
752 NASA/GSFC, Greenbelt, MD, 2014.

753 Huffman, G. J., Bolvin, D. T., Braithwaite D., Hsu K., Joyce R. , Kidd C., Nelkin Eric J., Sorooshian S., Tan J., and Xie  
754 P.: NASA Global Precipitation Measurement (GPM) Integrated Multi-satellitE Retrievals for GPM (IMERG),.  
755 [https://docserver.gesdisc.eosdis.nasa.gov/public/project/GPM/IMERG\\_ATBD\\_V06.pdf](https://docserver.gesdisc.eosdis.nasa.gov/public/project/GPM/IMERG_ATBD_V06.pdf), 2019.

756 Kim, H., Watanabe, S., Chang, E. C., Yoshimura, K., Hirabayashi, J., Famiglietti, J., and Oki, T.: Global Soil Wetness  
757 Project Phase 3 Atmospheric Boundary Conditions (Experiment 1) [Data set], Data Integration and Analysis System  
758 (DIAS), <https://doi.org/10.20783/DIAS.501>, 2017.

759 Kirchner, J. W.: Getting the right answers for the right reasons: Linking measurements, analyses, and models to advance  
760 the science of hydrology, *Water Resour. Res.*, 42(3), <https://doi.org/10.1029/2005WR004362>, 2006.

761 Klees, R., Revtova, E. A., Gunter, B.C. , Ditmar, P., Oudman, E., Winsemius H. C., and Savenije H.H.G.: The design of  
762 an optimal filter for monthly GRACE gravity models, *Geoph. J. Intern.*, 175 (2): 417–432,  
763 <https://doi.org/10.1111/j.1365-246X.2008.03922.x>, 2008

764 Kling, H., Fuchs, M., and Paulin, M.: Runoff conditions in the upper Danube basin under an ensemble of climate change  
765 scenarios, *J. Hydrol.*, 424, 264-277, <https://doi.org/doi:10.1016/j.jhydrol.2012.01.011>, 2012.

766 Landerer, F. W., and Swenson, S. C.: Accuracy of scaled GRACE terrestrial water storage estimates, *Water Resour. Res.*,  
767 48(4), <https://doi.org/10.1029/2011WR011453>, 2012.

768 Lehner, B., C. Reidy Liermann, C. Revenga, C. Vörösmarty, B. Fekete, P. Crouzet, P. Döll, M. Endejan, K. Frenken, J.  
769 Magome, C. Nilsson, J.C. Robertson, R. Rodel, N. Sindorf, and D. Wisser.: High-resolution mapping of the world's  
770 reservoirs and dams for sustainable river-flow management, *Front. Ecol. Environ.*, 9 (9): 494-502,  
771 <https://doi.org/10.1890/100125>, 2011.

772 Long, D., Longuevergne, L., and Scanlon, B. R.: Uncertainty in evapotranspiration from land surface modeling, remote  
773 sensing, and GRACE satellites, *Water Resour. Res.*, 50(2), 1131-1151, <https://doi.org/10.1002/2013WR014581>,  
774 2014.

775 Lorenz, C., H. Kunstmann, H., B. Devaraju, B., Tourian, M. J., N. Sneeuw, N., and J. Riegger, J.: Large-Scale Runoff  
776 from Landmasses: A Global Assessment of the Closure of the Hydrological and Atmospheric Water Balances,. *J.*  
777 *Hydrometeor.*, 15, 2111–2139, <https://doi.org/doi:10.1175/JHM-D-13-0157.1>, 2014.

778 Luthcke, S.B., Sabaka, T.J., Loomis, B.D., Arendt, A.A., McCarthy, J.J., and Camp, J.: Antarctica, Greenland and Gulf  
779 of Alaska land-ice evolution from an iterated GRACE global mascon solution, *J. Glaciol.*, Vol. 59, No. 216, 613-631,  
780 2013 <https://doi.org/doi:10.3189/2013JoG12J147>, 2013.

781 Massari, C., Brocca, L., Barbetta, S., Papathanasiou, C., Mimikou, M., and Moramarco, T.: Using globally available soil  
782 moisture indicators for flood modelling in Mediterranean catchments, *Hydrol. Earth Syst. Sci.*, 18(2), 839,  
783 <https://doi.org/10.5194/hess-18-839-2014>, 2014.

784 Massari, C., Brocca, L., Tarpanelli, A., Hong, Y., Crow, W., Ciabatta, L., Camici, S., Barbetta, S., and Moramarco, T.:  
785 Global surface runoff estimation in near real time by using SMAP and GPM, poster at SMAP conference, 2016.

786 Merz, R., and Blöschl, G.: A regional analysis of event runoff coefficients with respect to climate and catchment  
787 characteristics in Austria, *Water Resour. Res.*, 45(1), <https://doi.org/10.1029/2008WR007163>, 2009.

788 Mueller Schmied, H., Adam, L., Eisner, S., Fink, G., Flörke, M., Kim, H., ... and Song, Q.: Variations of global and  
789 continental water balance components as impacted by climate forcing uncertainty and human water use, *Hydrol. Earth*  
790 *Syst. Sci.*, 20(7), 2877-2898, <https://doi.org/10.5194/hess-20-2877-2016>, 2016.

791 Muneepeerakul, R., Azale, S., Botter, G., Rinaldo, A., and Rodriguez-Iturbe, I.: Daily streamflow analysis based on a  
792 two-scaled gamma pulse model, *Water Resour. Res.*, 46(11), <https://doi.org/10.1029/2010WR009286>, 2010.

793 Nash, J. E.: The form of the instantaneous unit hydrograph, IASH publication no. 45, 3–4, 114–121, 1957.

794 Natural Resources Conservation Service (NRCS): Urban hydrology for small watersheds, Tech. Release 55, 2nd ed., U.S.  
795 Dep. of Agric., Washington, D. C. (available at [ftp://ftp.wcc.nrcs.usda.gov/downloads/](ftp://ftp.wcc.nrcs.usda.gov/downloads/hydrology_hydraulics/tr55/tr55.pdf)  
796 [hydrology\\_hydraulics/tr55/tr55.pdf](ftp://ftp.wcc.nrcs.usda.gov/downloads/hydrology_hydraulics/tr55/tr55.pdf)), 1986.

797 Orth, R., and Seneviratne, S. I.: Introduction of a simple-model-based land surface dataset for Europe, *Environ. Res. Lett.*,  
798 10(4), 044012, <https://doi.org/10.1088/1748-9326/10/4/044012>, 2015.

799 Pellet, V., Aires, F., Munier, S., Fernández Prieto, D., Jordá, G., Dorigo, W. A., ... and Brocca, L.: Integrating multiple  
800 satellite observations into a coherent dataset to monitor the full water cycle—application to the Mediterranean region.,  
801 *Hydrol. Earth Syst. Sci.*, 23(1), 465-491, <https://doi.org/10.5194/hess-23-465-2019>, 2019.

802 Prudhomme, C., Giuntoli, I., Robinson, E. L., Clark, D. B., Arnell, N. W., Dankers, R., ... and Hagemann, S.: Hydrological  
803 droughts in the 21st century, hotspots and uncertainties from a global multimodel ensemble experiment, *Proceedings*  
804 *of the National Academy of Sciences*, 111(9), 3262-3267, 2014.

805 Rakovec, O., Kumar, R., Attinger, S., and Samaniego, L.: Improving the realism of hydrologic model functioning through  
806 multivariate parameter estimation, *Water Resour. Res.*, 52(10), 7779-7792, <https://doi.org/10.1002/2016WR019430>,  
807 2016.

808 Richards, L.A.: Capillary conduction of liquids through porous mediums, *Physics*. 1 (5): 318–333.,  
809 Bibcode:1931Physi.1.318R., <https://doi.org/doi:10.1063/1.1745010>, 1931.

810 Riegger, J., and Tourian, M. J.: Characterization of runoff-storage relationships by satellite gravimetry and remote  
811 sensing, *Water Resour. Res.*, 50, 3444–3466, <https://doi.org/doi:10.1002/2013WR013847>, 2014.

812 Rodell, M., Beaudoin, H. K., L’Ecuyer, T. S., Olson, W. S., Famiglietti, J. S., Houser, P. R., Adler, R., Bosilovich, M.  
813 G., Clayson, C. A., Chambers, D., Clark, E., Fetzer, E. J., Gao, X., Gu, G., Hilburn, K., Huffman, G. J., Lettenmaier,  
814 D. P., Liu, W. T., Robertson, F. R., Schlosser, C. A., Sheffield, J. and Wood, E. F.: The observed state of the water  
815 cycle in the early 15twenty-first century, *J. Clim.*, 28(21), 8289–8318, <https://doi.org/doi:10.1175/JCLI-D-14-00555.1>, 2015.

816 Schellekens, J., Dutra, E., Martínez-de la Torre, A., Balsamo, G., van Dijk, A., Sperna Weiland, F., Minvielle, M., Cal-  
817 vet, J.-C., Decharme, B., Eisner, S., Fink, G., Flörke, M., Peßenteiner, S., van Beek, R., Polcher, J., Beck, H., Orth, R.,  
818 Calton, B., Burke, S., Dorigo, W., and Weedon, G. P.: A global water resources ensemble of hydrological models: the  
819 earth2Observe Tier-1 dataset, *Earth Syst. Sci. Data*, 9, 389–413, <https://doi.org/10.5194/essd-9-389-2017>, 2017.

820 Schwanghart, W., and Kuhn, N. J.: TopoToolbox: A set of Matlab functions for topographic analysis., *Environ. Model.*  
821 *Softw. Environmental Modelling & Software*, 25(6), 770-781, 2010.

822 Seneviratne, S. I., Corti, T., Davin, E. L., Hirschi, M., Jaeger, E. B., Lehner, I., ... and Teuling, A. J.: Investigating soil  
823 moisture–climate interactions in a changing climate: A review, *Earth-Sci. Rev.*, 99(3-4), 125-161,  
824 <https://doi.org/10.1016/j.earscirev.2010.02.004>, 2010.



826 Sneeuw, N., Lorenz, C., Devaraju, B., Tourian, M. J., Riegger, J., Kunstmann, H., and Bárdossy, A.: Estimating runoff  
827 using hydro-geodetic approaches, *Surv. Geophys.*, 35(6), 1333-1359, <https://doi.org/10.1007/s10712-014-9300-4>,  
828 2014.

829 Solomatine, D. P., and Ostfeld, A.: Data-driven modelling: some past experiences and new approaches, *J. Hydroinform.*,  
830 10(1), 3-22, <https://doi.org/10.2166/hydro.2008.015>, 2008.

831 Strahler, A. N.: Hypsometric (area-altitude) analysis of erosional topography, *Geol. Soc. Am. Bull.* Geological Society of  
832 America Bulletin, 63(11), 1117-1142, [https://doi.org/10.1130/0016-7606\(1952\)63\[1117:HAAOET\]2.0.CO;2](https://doi.org/10.1130/0016-7606(1952)63[1117:HAAOET]2.0.CO;2), 1952.

833 Tapley, B.D., Watkins, M.M., Flechtner, F. et al.: Contributions of GRACE to understanding climate change, *Nat. Clim.*  
834 *Chang.*, 9, 358–369, <https://doi.org/doi:10.1038/s41558-019-0456-2>, 2019.

835 Thiemig, V., Rojas, R., Zambrano-Bigiarini, M., and De Roo, A.: Hydrological evaluation of satellite rainfall estimates  
836 over the Volta and Baro-Akobo Basin, *J. Hydrol.*, 499, 324-338, <https://doi.org/10.1016/j.jhydrol.2013.07.012>, 2013.

837 Tourian, M. J., Reager, J. T., and Sneeuw, N.: The total drainable water storage of the Amazon river basin: A first estimate  
838 using GRACE, *Water Resour. Res.*, 54, <https://doi.org/10.1029/2017WR021674>, 2018.

839 Trambly, Y., Bouvier, C., Martin, C., Didon-Lescot, J. F., Todorovik, D., and Domergue, J. M.: Assessment of initial  
840 soil moisture conditions for event-based rainfall–runoff modelling, *J. Hydrol.*, 387(3-4), 176-187,  
841 <https://doi.org/10.1016/j.jhydrol.2010.04.006>, 2010.

842 Troutman, B. M., and Karlinger, M.B.: Unit hydrograph approximation assuming linear flow through topologically  
843 random channel networks, *Water Resour. Res.*, 21, 743 – 754, <https://doi.org/doi:10.1029/WR021i005p00743>, 1985.

844 Vörösmarty C. J., and Coauthors: Global water data: A newly endangered species, *Eos, Trans. Amer. Geophys. Union*,  
845 82, 54, <https://doi.org/10.1029/01EO00031>, 2002.

846 Vose, R.S., Applequist, S., Durre, I., Menne, M.J., Williams, C.N., Fenimore, C., Gleason, K., and Arndt, D.: Improved  
847 Historical Temperature and Precipitation on Time Series For U.S. Climate Divisions., *J. Meteorol. and Climat.*,  
848 53(May), 1232–1251, <https://doi.org/10.1175/JAMC-D-13-0248.1> DOI: 10.1175/JAMC-D-13-0248.1, 2014.

849 Wagner, W., Blöschl, G., Pampaloni, P., Calvet, J. C., Bizzarri, B., Wigneron, J. P., and Kerr, Y.: Operational readiness  
850 of microwave remote sensing of soil moisture for hydrologic applications, *Hydrol. Res.*, 38(1), 1-20,  
851 <https://doi.org/10.2166/nh.2007.029>, 2007.

852 Wagner, W., Lemoine, G., and Rott, H.: A method for estimating soil moisture from ERS scatterometer and soil data.,  
853 *Remote Sens. Environ. Remote Sensing of Environment*, 70, 191–207, [https://doi.org/doi:10.1016/S0034-4257\(99\)00036-X](https://doi.org/doi:10.1016/S0034-4257(99)00036-X), 1999.

855 Wisser, D., Fekete, B. M., Vörösmarty, C. J., and Schumann, A. H.: Reconstructing 20th century global hydrography: a  
856 contribution to the Global Terrestrial Network- Hydrology (GTN-H), *Hydrol. Earth Syst. Sci.*, 14, 1–24,  
857 <https://doi.org/doi:10.5194/hess-14-1-2010>, 2010.

858 Yokoo, Y., and Sivapalan, M.: Towards reconstruction of the flow duration curve: Development of a conceptual  
859 framework with a physical basis, *Hydrol. Earth Syst. Sci.*, 15(9), 2805–2819, [https://doi.org/10.5194/hess-15-2805-](https://doi.org/10.5194/hess-15-2805-2011)  
860 [2011](https://doi.org/10.5194/hess-15-2805-2011), 2011.

861 Zhang, Y., Pan, M., Sheffield, J., Siemann, A. L., Fisher, C. K., Liang, M., ... and Zhou, T.: A Climate Data Record  
862 (CDR) for the global terrestrial water budget: 1984–2010, *Hydrol. Earth Syst. Sci.*, 22, 241–263,  
863 <https://doi.org/10.5194/hess-22-241-2018>(Online), 22(PNNL-SA-129750), 2018.



865 Table 1. Location of gauging stations over the Mississippi basins and upstream contributing area.  
866 Bold text is used to indicate stations where the STREAM v1.3 model has been calibrated.

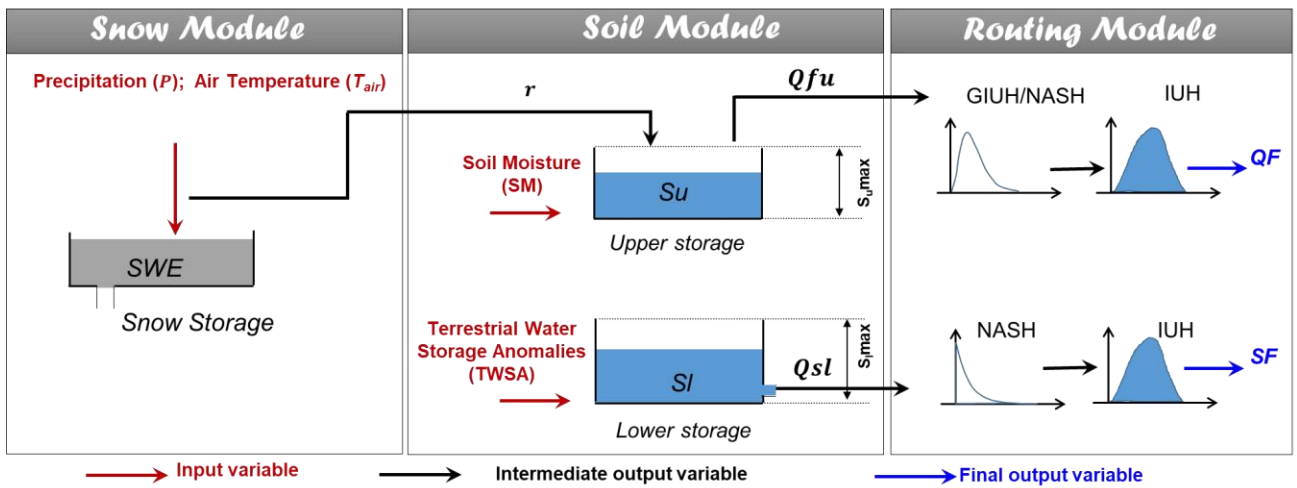
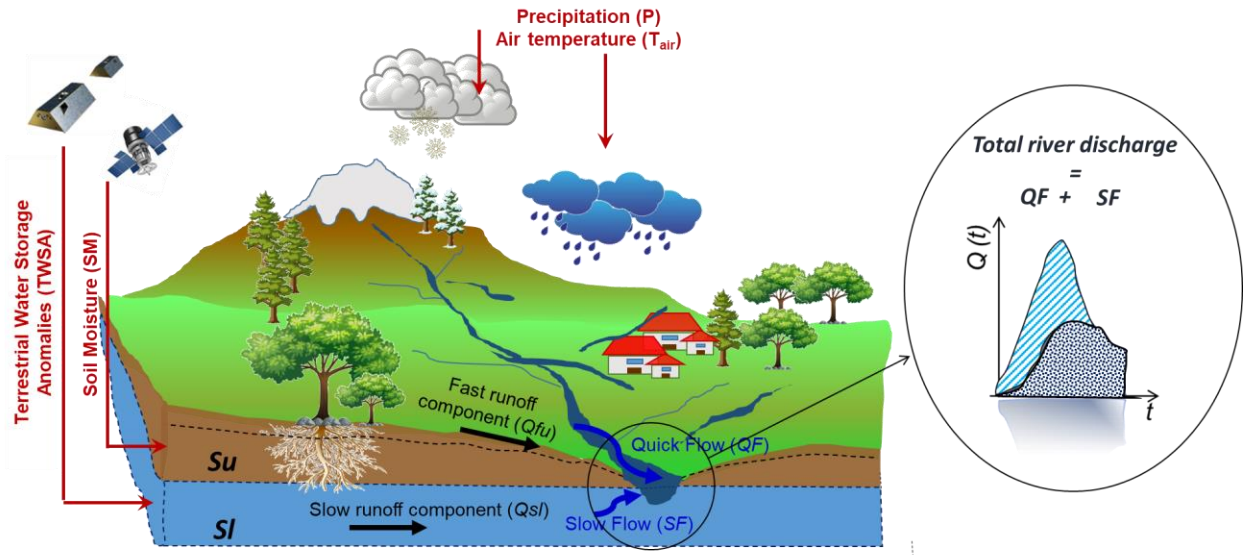
#	River	Station name	Latitude (°)	Longitude (°)	Upstream area (km <sup>2</sup> )	Mean annual river discharge (m <sup>3</sup> /s)	Presence of dam
1	Missouri	Bismarck, ND	-100.82	46.81	481'232	633	Garrison dam
2	Missouri	Omaha, NE	-95.92	41.26	814'371	914	Gavins Point Dam
3	Missouri	Kansas City, MO	-94.59	39.11	1'229'427	1499	---
4	<b>Missouri</b>	<b>Hermann, MO</b>	<b>-91.44</b>	<b>38.71</b>	<b>1'330'000</b>	<b>2326</b>	---
5	Kansas	Wamego, KS	-96.30	39.20	143'054	141	Kanopolis
6	<b>Mississippi</b>	<b>Keokuk, IA</b>	<b>-91.37</b>	<b>40.39</b>	<b>282'559</b>	<b>1948</b>	---
7	Rock	Near Joslin, IL	-90.18	41.56	23'835	199	---
8	Mississippi	Chester, IL	-89.84	37.90	1'776'221	6018	---
9	Arkansas	<b>Murray Dam Near Little Rock, AR</b>	<b>-92.36</b>	<b>34.79</b>	<b>408'068</b>	<b>1249</b>	---
10	<b>Mississippi</b>	<b>Vicksburg, MS</b>	<b>-90.91</b>	<b>32.32</b>	<b>2'866'590</b>	<b>17487</b>	---
11	<b>Ohio</b>	<b>Metropolis, ILL.</b>	<b>-88.74</b>	<b>37.15</b>	<b>496'134</b>	<b>7931</b>	---

867  
868

869 Table 2. Performance scores obtained over the Mississippi river sections during the calibration and  
870 validation periods.

#	CALIBRATION PERIOD			VALIDATION PERIOD		
SCORE	KGE (-)	R (-)	RRMSE (%)	KGE (-)	R (-)	RRMSE (%)
CALIBRATED SECTIONS						
10	0.78	0.78	30	0.74	0.80	38
9	0.62	0.75	71	0.67	0.85	77
6	0.83	0.84	39	0.73	0.84	46
4	0.77	0.78	46	0.72	0.75	50
11	0.82	0.82	44	0.70	0.86	51
SECTIONS NOT USED FOR CALIBRATION						
1	-3.26	0.08	137	0.20	0.44	96
2	-0.57	0.48	118	0.40	0.53	89
3	0.16	0.71	83	0.39	0.70	72
5	-1.49	0.24	368	-1.26	0.31	358
7	0.53	0.68	71	0.20	0.70	81
8	0.80	0.84	36	0.77	0.84	39

871  
872

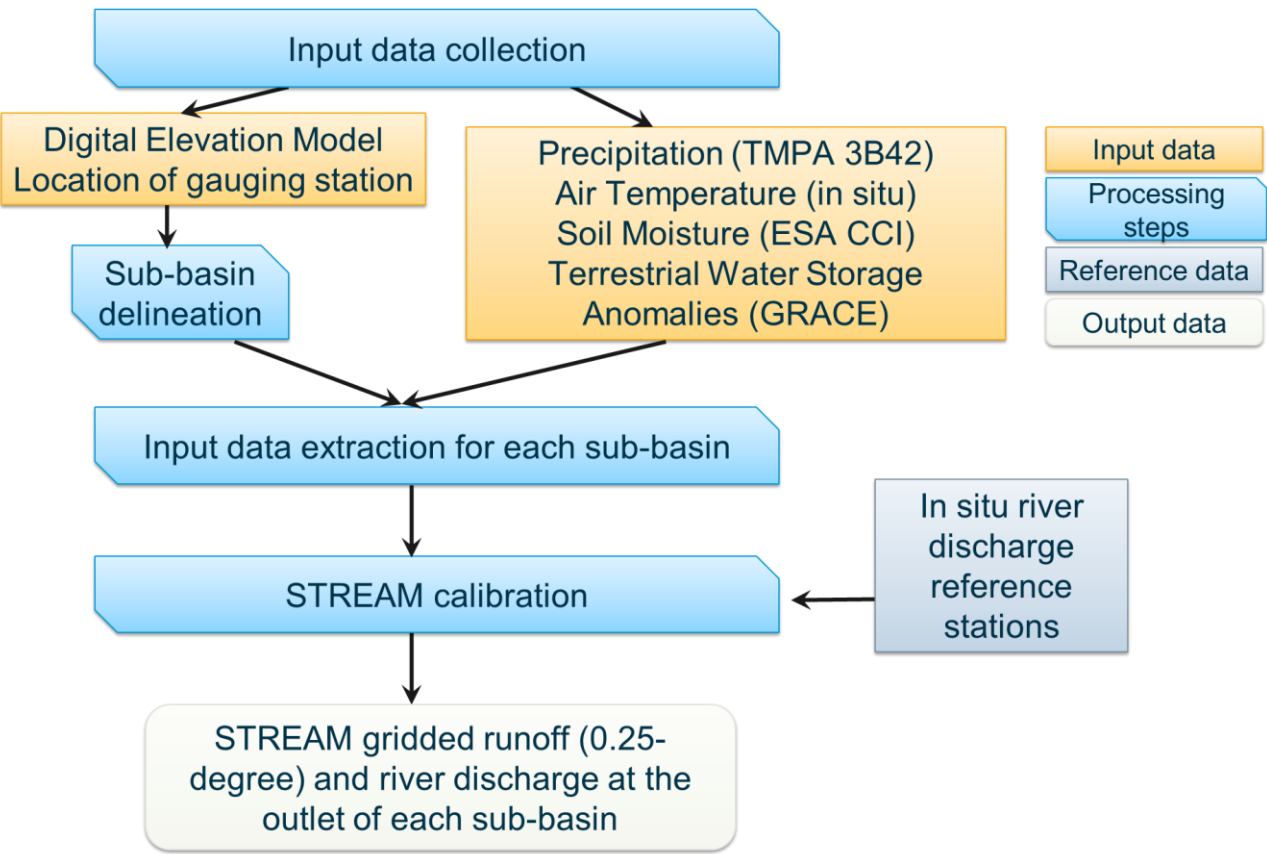


873

874 Figure 1. Configuration of the STREAM v1.3 model adopted for total runoff estimation. The model  
 875 includes three modules, the snow module allowing to separate snowfall from precipitation, the soil  
 876 module that simulates the slow and quick runoff components ( $Q_{su}$  and  $Q_{fu}$ , respectively) and the  
 877 routing module for flood simulation. Red arrows indicate input variables; black arrows indicate  
 878 intermediate output variables; blue arrows indicate final output variables. The components  $Q_{fu}$  and  
 879  $Q_{su}$  are computed by using satellite  $P$ , soil moisture and TWSA data as input to the soil module.  
 880 Please refer to text for symbols.

881

882



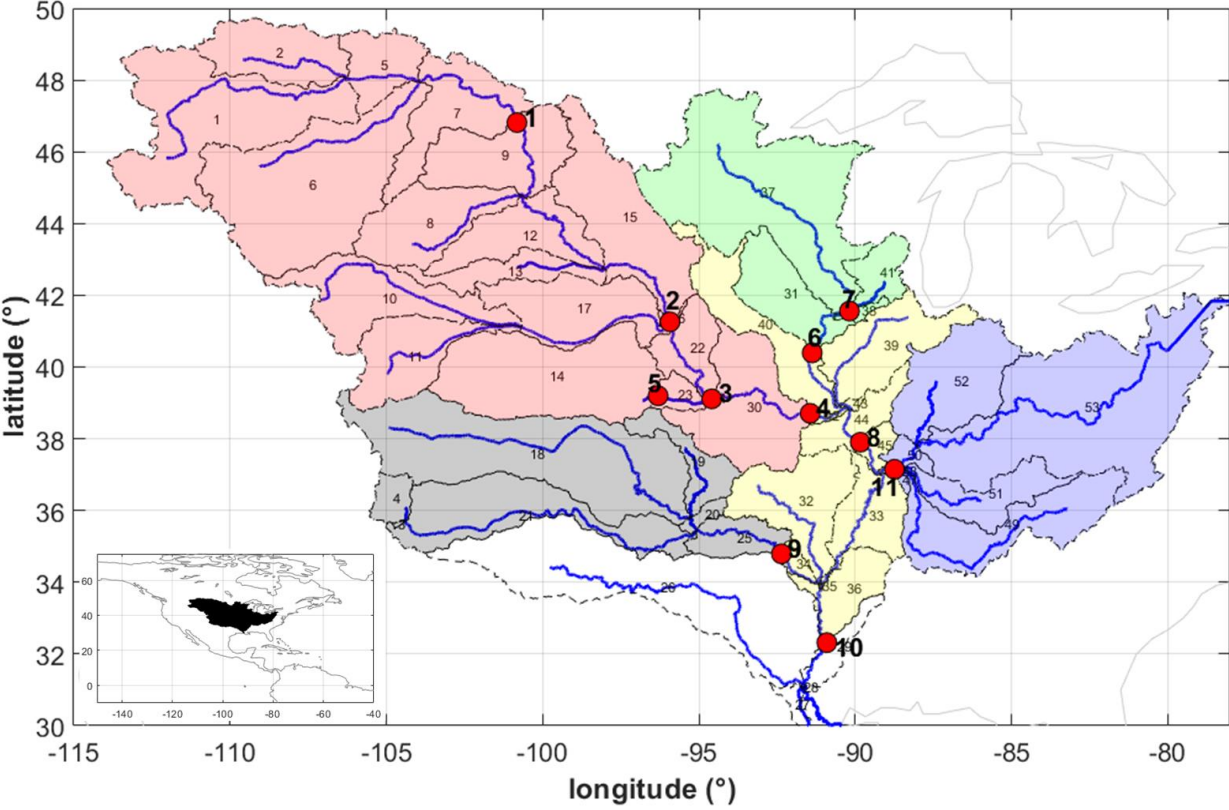
883

884

885 Figure 2. Processing steps of the STREAM v1.3 model.

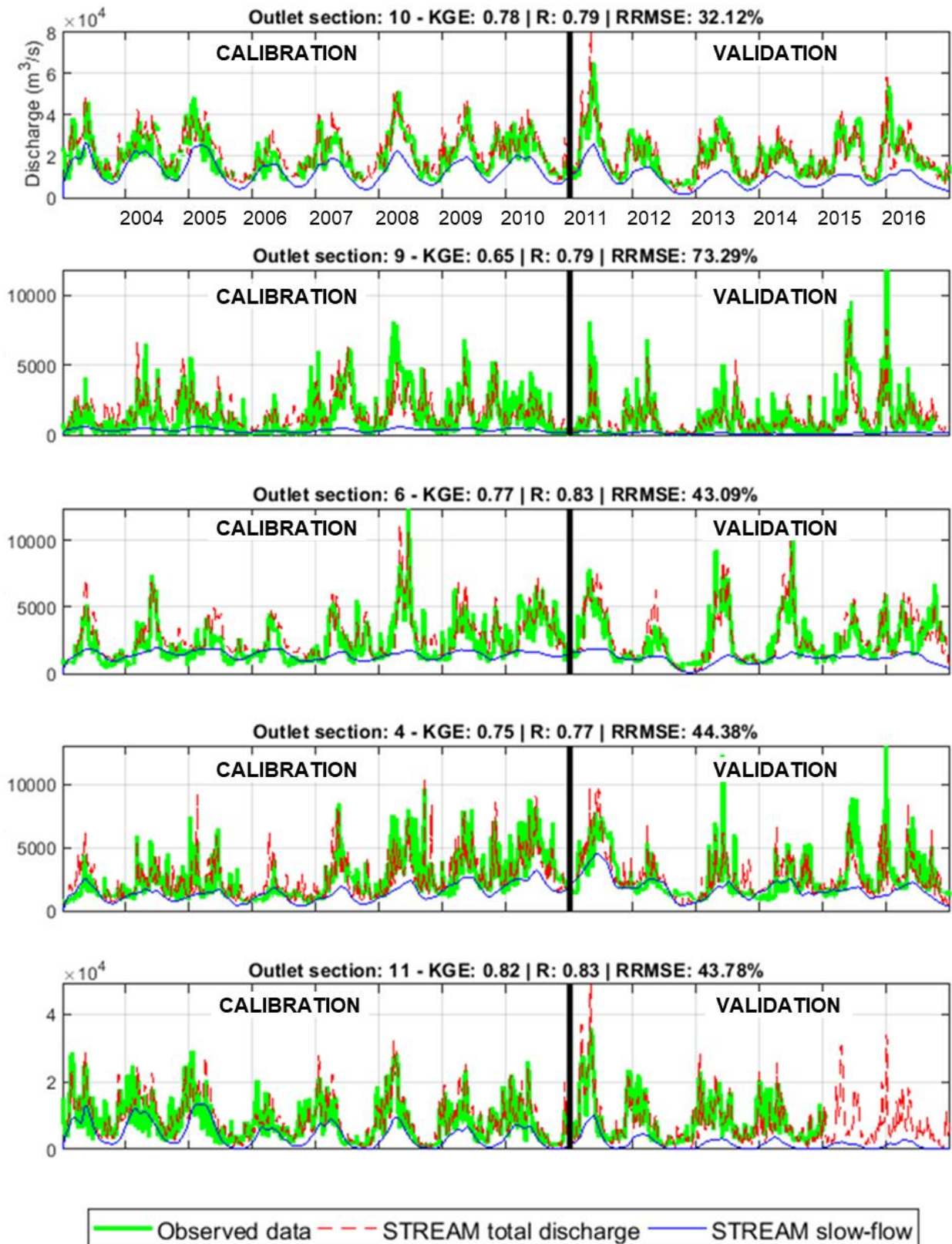
886

887



888

889 Figure 3. Mississippi sub-basin delineation. Red dots indicate the location of the discharge gauging  
890 stations; different colours identify different inner sections (and the related contributing sub-basins)  
891 used for the model calibration.  
892

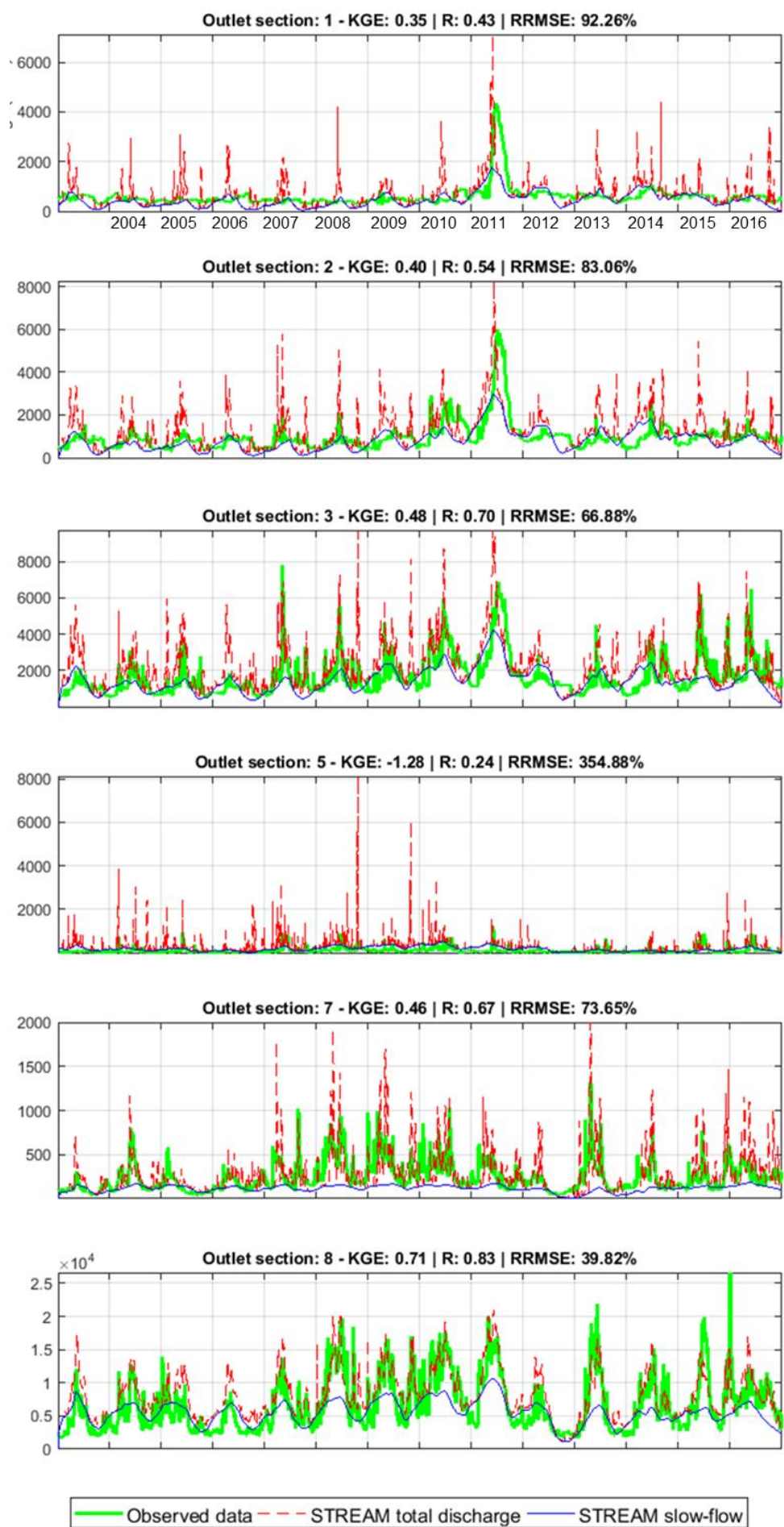


893

894 Figure 4. Comparison between observed and simulated river discharge time series over the five  
 895 calibrated sections over Mississippi river basin. Performance scores at the top of each plot refer to  
 896 the entire study period (2003–2016).

897

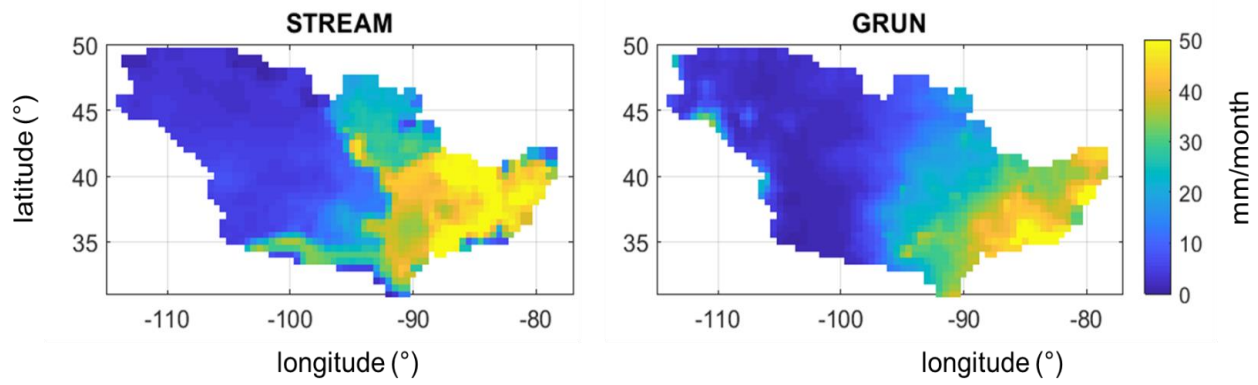




800  
901  
902  
903  
904

Figure 5. Comparison between observed and simulated river discharge time series over the gauged sections not used in the calibration phase. Performance scores at the top of each plot refer to the entire study period (2003–2016).





905

906 Figure 6. Mississippi river basin: mean monthly runoff for the period 2003–2014 obtained by  
907 STREAM v1.3 and GRUN models.

908

910    Table 1A. Description of STREAM v1.3 parameters, belonging module, variability range and unit.

Parameter	Description	Module	Range Variability	Unit
Cm	degree-day coefficient	Snow	0.1/24-3	[-]
$\alpha$	exponent of infiltration	Soil	1-30	[-]
T	characteristic time length	Soil	0.01-80	[days]
$\beta$	coefficient relationship slow runoff component and TWSA	Soil	0.1-20	[mm h-1]
m	exponent in the relationship between slow runoff component and TWSA	Soil	1-15	[-]
$\gamma$	parameter of GIUH	Routing	0.5-5.5	[-]
C	Celerity	Routing	1-60	[km h-1]
D	Diffusivity	Routing	1-30	[km2 h-1]

911